## Report No. 24/2025

DOI: 10.4171/OWR/2025/24

## Mathematical Advances in Geophysical Fluid Dynamics

Organized by
Anne-Laure Dalibard, Paris
Peter Korn, Hamburg
Leslie M. Smith, Madison
Edriss S. Titi, Cambridge UK/College Station/Rehovot

11 May - 16 May 2025

ABSTRACT. The workshop "Mathematical Advances in Geophysical Fluid Dynamics" addressed recent advances in modeling, analytical, computational and stochastical studies of geophysical models. In particular addressed are atmosphere-, ocean- and sea-ice models, well-posedness and analysis of relevant geophysical fluid regimes and models, including stochastically forced equations, boundary layers as well as coupled models.

Mathematics Subject Classification (2020): 76-XX, 86A10, 35-XX, 60Hxx.

License: Unless otherwise noted, the content of this report is licensed under CC BY SA 4.0.

## Introduction by the Organizers

This workshop was dedicated to the investigation of geophysical models for atmosphere, ocean and sea-ice by means of mathematical analysis, numerical simulations and physical reasoning. The mathematical investigation of geophysical flows involves many modern techniques from analysis, stochastics and computation.

Of special interest are the regularity properties of solutions of the associated systems of equations, the implications of convex integration method for fluid dynamical systems and turbulence and consequences for a suitable notion of solution for geophysical equations. An active research topic is the rigorous mathematical understanding of various sea-ice models. The analysis coupled atmosphere-sea ice-ocean models remains a formidable challenge. New analytical and computational tools are being developed in order to analyze models from moist atmospheric dynamics including phase transitions and particular geophysical phenomena such as cyclones and Saturn's hexagon.

A key feature of this workshop was bringing together leading experts form various communities and therefore from diverse scientific backgrounds such as analysis, modeling, numerics and computations as well as stochastic analysis. The lectures presented took 40 minutes which were followed by lively and interactive discussions for about 15 minutes. Shorter presentations were provided, lasting around 15 minutes each. Evening sessions attracted special attention, where graduate students as well as postdoctoral fellows gave excellent presentations about their research work. The presence of early career participants and gender diversity was very visible during the meeting. The workshop also aimed to encourage early career participants to play an important role in this area of research. The meeting ignited lively discussions and exchange of ideas. One plenary session gave rise to animated discussions on fundamental matters regarding research on theoretical fluid mechanics and geophysical models. We are convinced that the scientific exchange between the participants will lead to many exciting new developments and collaborations.

# Workshop: Mathematical Advances in Geophysical Fluid Dynamics

## **Table of Contents**

Rupert Klein (joint with Tom Dörffel, Sabine Doppler, Boualem Khouider)  Triple-deck theory for the control of convection in idealized axisymmetric tropical storms
Samuel N. Stechmann (joint with Antoine Remond-Tiedrez, Leslie M. Smith)  Beyond linear decomposition: a nonlinear eigenspace decomposition for the slow and fast components of a moist atmosphere with clouds 1222
Boualem Khouider (joint with Clint Seinin, Sofiane Chatta, Salim Bensasi, Tahar Boulmezaoud)  Progress in the analytical and numerical studies of the Hibler model of sea-ice dynamics
Matthias Hieber (joint with A. Agresti, T. Binz, F. Brandt, A. Hussein, M. Saal, T. Zöchling)  The primitive equations subject to deterministic and stochastic forces 1228
Sophie Thery Well-posedness of a non-local Ocean-Atmosphere coupling model 1229
Daniel Bäumer (joint with Rupert Klein, Norbert J. Mauser)  Scaling regimes for moist atmospheric flows and the Clausius-Clapeyron relation
Felix Brandt (joint with Sunčica Čanić, Boris Muha)  Finite energy weak solutions to a multilayered 3D fluid-poroelastic structure interaction problem
Lucas Huysmans  Mixing Estimates for Passive Scalar Transport by Sobolev and BV Vector  Fields
László Székelyhidi Jr. (joint with Jan Burczak and Bian Wu)  Advection by turbulent velocity fields
Carolin Mehlmann  Numerical aspects of simulating large-scale sea-ice dynamics1236
Marita Thomas (joint with Xin Liu, Edriss Titi)  Analysis of a viscoplastic Burgers equation
Emmanuel Dormy (joint with Peter A. Davidson, Kerry A. Emanuel, Ludivine Oruba and Andrew M. Soward)  Eye formation in tropical cyclones

Amru Hussein (joint with Ken Furukawa, Yoshikazu Giga, Matthias Hieber, Takahito Kashiwabara, Marc Wrona)  The three limits of the hydrostatic approximation
Yasunori Maekawa (joint with Sameer Iyer)  On the stationary triple-deck equations
Daniel W. Boutros (joint with Xin Liu, Marita Thomas and Edriss S. Titi)  Mathematical analysis of an inviscid Voigt regularisation of the elastic-viscous-plastic sea-ice model
Dongjuan Niu (joint with Huiru Wu, Robin Ming Chen, Houzhi Tang)  Analysis aspect of tropical climate model
Ruiao Hu (joint with Theo Diamantakis, James-Michael Leahy)  Variational Closures Of Composite Homogenised Fluid Flows1246
Oliver D. Street  Stochastic geometric mechanics and its application to transport noise in continuum dynamics
Jörg Weber  Traveling water waves
Adrian Constantin (joint with R. S. Johnson)  On the nonlinear dynamics of Saturn's hexagon
Felix Otto (joint with Sefika Kuzgun, Peter Morfe, Christian Wagner)  Critical Drift-Diffusion equations: Intermittent behavior
Simon Markfelder (joint with Valentin Pellhammer, Christian Klingenberg, Emil Wiedemann)  What are good solution concepts for the PDEs of fluid mechanics? 1253
Yanqiu Guo (joint with Mohammad Abu Hamed, Ciprian G. Gal, Michael Ilyin, Edriss S. Titi)  Inertial Manifolds for Regularized Navier-Stokes Equations
Laura Cope (joint with Peter H. Haynes)  The Dynamics of Stochastically-Forced Beta-Plane Zonal Jets
Susanna V. Haziot (joint with Claudia García)  Global bifurcation for corotating vortex patches
Basile Gallet  Two-dimensional turbulence above topography: condensation transition and selection of minimum enstrophy solutions
Marcel Oliver  Optimal Balance – A black-box method for fast-slow decompositions of fluid flow

~ ~	_	
Yann	$\mathrm{Br}_{\mathcal{C}}$	nier

### Abstracts

## Triple-deck theory for the control of convection in idealized axisymmetric tropical storms

Rupert Klein

(joint work with Tom Dörffel, Sabine Doppler, Boualem Khouider)

Recent work by some of the authors [1] showed that the classical decomposition of mid-latitude flows into the quasi-geostrophic bulk and Ekman layer flows (QG-Ekman) cannot capture important diabatic effects in the lower 1-5 km associated, e.g., with thermal convection or cloud processes. Their remedy is an extension of QG-Ekman theory by a third "diabatic layer" (DL) of intermediate height (QG-DL-Ekman theory).

The present work demonstrates that a similar asymptotic triple-deck expansion for vortices in gradient wind balance enables the theoretical explanation of several important observational features of tropical storms and incipient hurricanes and typhoons. For instance, super-gradient winds are naturally found in the friction layer (FL), and the newly introduced intermediate layer hosts the lifting condensation level (LCL) and the level of free convection (LFC) and, possibly, a convective inhibition layer (CIN). Due to its significance for the onset of convective processes that feed back into the primary circulation, this intermediate layer is labeled "convection controlling layer" (CCL) here.

As the most significant finding of this work, it is revealed how angular momentum transport between the three layers induces vortex intensification. Additionally, we give details on how multiscale convection and the associated entrainment of mass in the transition zone between the CCL and the bulk tropospheric flow (bulk) are the keys to spinning up the boundary layer flow. The hydrostatic and gradient wind balances, upward (FL  $\rightarrow$  CCL) control of angular momentum, sensible heat, and moisture, and buoyancy instabilities with positive CAPE (convectively available potential energy) throughout the middle troposphere all interact in controlling vortex spin-up at the interface between the bulk vortex and the convection controlling layer.

This work addresses upright axisymmetric vortices, while asymmetries, associated among other things with strong vortex tilt as in the bulk tilted vortex theory of [2, 3], are deferred to future studies.

- [1] Klein R., Schielicke L., Pfahl S., Khouider B., QG-DL-Ekman: Dynamics of a diabatic layer in the quasi-geostrophic framework, J. Atmos. Sci., 79(3), 887–905 (2022); arXiv:2104.10598
- [2] Päschke E., Marschalik P., Owinoh A.Z., Klein R., Motion and structure of atmospheric mesoscale baroclinic vortices: dry air and weak environmental shear, J. Fluid Mech., 701, 137–170, (2012)
- [3] Dörffel T., Papke A., Klein R., Ernst N., Smolarkiewicz P.K., Dynamics of tilted atmospheric vortices under asymmetric diabatic heating, TCFD, 35, 831–873, (2021)

Beyond linear decomposition: a nonlinear eigenspace decomposition for the slow and fast components of a moist atmosphere with clouds

(joint work with Antoine Remond-Tiedrez, Leslie M. Smith)

Decomposing a vector field, or a state vector, into several constitutive components is ubiquitous in fluid mechanics and atmospheric science. For example, the Helmholtz decomposition will split a vector field into its potential and divergence-free components, and it is used throughout fluid mechanics. Another example is the vortical—wave decomposition of a state vector which is used in atmospheric and oceanic sciences to understand the fast rotation and strong stratification regime of the Boussinesq equations, e.g., [3]. Crucially, both of these decompositions can be viewed from multiple perspectives and share salient features such as reconstruction of the original field via elliptic partial differential equations (PDEs), a rich geometric interpretation of the decomposition (involving orthogonality and projections), and a connection to slow and fast components of appropriate dynamical systems.

In this paper we consider a moist Boussinesq system from atmospheric dynamics, which brings additional realism and complexity due to clouds. We ask the following question: does this moist, cloudy Boussinesq system also admit such a decomposition?

While these decompositions have applications in slow–fast dynamical systems, they can be investigated without reference to the dynamical evolution, by considering the associated operator. To see this from a general perspective, consider a dynamical system written abstractly as

$$\partial_t U + \frac{1}{\epsilon} \mathcal{D}_0 U + \mathcal{D}_1 U = 0,$$

where  $\epsilon$  is a small parameter,  $\mathcal{D}_0$  is the leading-order operator, and  $\mathcal{D}_1$  is the next-order contribution to the operator for the dynamical system. To leading order with respect to  $\epsilon$ , it is the operator  $\mathcal{D}_0$  that contains the essential information. Understanding the dynamics can be tantamount to understanding the operator  $\mathcal{D}_0$ . Hence, in the remainder of the paper, we will seldom refer to the actual dynamical evolution, and instead the main object of interest is the operator  $\mathcal{D}_0$ .

In past cases, such as the Helmholtz decomposition or Boussinesq equations, the leading-order operator is linear ( $\mathcal{D}_0 = \mathcal{L}$ ), and the decomposition involves a linear operator and linear eigenmodes. On the other hand, for an atmosphere with clouds, additional nonlinearity arises from phase changes of water, and  $\mathcal{D}_0 = \mathcal{N}$  is a nonlinear operator. Hence a substantial challenge in the present paper is from nonlinearity, from the distinction

(1) 
$$\mathcal{D}_0 = \mathcal{L} \quad \text{versus} \quad \mathcal{D}_0 = \mathcal{N}.$$

For a nonlinear operator, it is not clear if eigenmodes can be identified. Consequently, a decomposition

$$(2) U = U_1 + U_2 + U_3 + \cdots$$

into all of the eigenmodes is likely to be impossible.

Despite the challenges of nonlinearity in (1)–(2), here we forge ahead with a decomposition in the spirit of (2) as the main aim and main theme.

The moist Boussinesq system, with stratification and rotation (i.e. the Coriolis effect), is

(3) 
$$\partial_t u + u \cdot \nabla u + \frac{1}{\varepsilon} (e_3 \times u + \nabla p - \theta e_3) = 0,$$

(4) 
$$\partial_t \theta + u \cdot \nabla \theta + \frac{\Gamma_\theta}{\varepsilon} u_3 = C,$$

(5) 
$$\partial_t q_v + u \cdot \nabla q_v - \frac{\Gamma_q}{\varepsilon} u_3 = -C \text{ and }$$

$$\partial_t q_l + u \cdot \nabla q_l = C,$$

subject to  $\nabla \cdot u = 0$ . In comparison to the dry Boussinesq system, the moist Boussinesq system includes additional evolution equations for the water vapor mixing ratio,  $q_v$ , in (5) and for the liquid water mixing ratio,  $q_l$ , in (6). It also includes a source/sink term C for condensation and evaporation, which represent phase changes between the vapor and liquid phases of water, and associated heating and cooling. The constants  $\Gamma_{\theta}$  and  $\Gamma_{q}$  correspond to parameters encoding the strength of the background vertical gradients in potential temperature and water vapor, respectively. While additional cloud microphysics processes will not be considered here, the moist Boussinesq system above is valuable for more complex scenarios as well, since it provides the starting point for extensions that include rainfall, ice, other precipitation, and other complexities [1, 5, 6].

Next it is convenient to rewrite the moist Boussinesq system in a way that the source terms C in (4)–(6) do not explicitly appear, through a convenient change of variables. This reformulation has been used in several past studies and has facilitated theoretical advances such as an energy decomposition [5, 4] and conservation of potential vorticity [2], even in the presence of clouds and phase changes.

For the convenient way of rewriting (3)–(6), we transform to a different set of thermodynamic variables that is conserved. In particular, define the equivalent potential temperature,  $\theta_e$ , and total water mixing ratio,  $q_t$ , as  $\theta_e = \theta + q_v$  and  $q_t = q_v + q_l$ . The evolution equations of  $\theta_e$  and  $q_t$  can be found by taking appropriate linear combinations of (4)–(6). To complete the rewriting, the buoyancy term  $\theta/\epsilon$  from (3) must also be rewritten in terms of  $\theta_e$  and  $q_t$ .

The end result of the rewriting is the moist Boussinesq system in the following form:

(7) 
$$\partial_t u + u \cdot \nabla u + \frac{1}{\varepsilon} (e_3 \times u + \nabla p - (\theta_e - \min_0 q_t) e_3) = 0,$$

(8) 
$$\partial_t \theta_e + u \cdot \nabla \theta_e = -\frac{1}{\varepsilon} u_3 \text{ and}$$

(9) 
$$\partial_t q_t + u \cdot \nabla q_t = \frac{1}{\varepsilon} u_3,$$

subject to  $\nabla \cdot u = 0$ . An important feature is that the source term of condensation and evaporation, C, has been eliminated. The nonlinearity due to clouds appears now in the buoyancy term  $\theta/\epsilon$  from (3) which has been rewritten in terms of  $\theta_e$  and  $q_t$ . The notation  $\min_0 q_t = \min(0, q_t)$  has been introduced in (7), and the saturation water vapor parameter  $q_{vs}$  has been set to zero without loss of generality, and for simplicity. Also we have now set the background gradient parameters from (4) and (5) to be  $\Gamma_{\theta} = 2$  and  $\Gamma_{q} = 1$  without loss of generality within the stably stratified regime, and for simplicity.

The key challenge with this system is that nonlinearities are present in the leading order,  $\mathcal{D}_0 = \mathcal{N}$ , at  $O(\epsilon^{-1})$ , due to phase boundaries at cloud edge. Therefore standard tools of linear algebra, relying on eigenvalues and eigenvectors, are not applicable. The question we address in this paper is this: in spite of the nonlinearities, can we find a decomposition for this moist Boussinesq system?

We identify such a decomposition adapted to the nonlinear balances arising from water phase boundaries. This decomposition combines perspectives from partial differential equations (PDEs), the geometry, and the conserved energy. This decomposition may be important in applications because, like its linear counterparts, it may be used to analyze observational data. Moreover, by contrast with previous decompositions, its formulation includes the nonlinearity from the presence of clouds.

- R. Klein and A. J. Majda. Systematic multiscale models for deep convection on mesoscales. Theor. Comput. Fluid Dyn., 20:525-551, 2006.
- [2] P. Kooloth, L. M. Smith, and S. N. Stechmann. Hamilton's principle with phase changes and conservation principles for moist potential vorticity. *Quarterly Journal of the Royal Meteorological Society*, 149(752):1056-1072, 2023.
- [3] A. Majda. Introduction to PDEs and waves for the atmosphere and ocean, volume 9 of Courant Lecture Notes in Mathematics. New York University, Courant Institute of Mathematical Sciences, New York; American Mathematical Society, Providence, RI, 2003.
- [4] D. H. Marsico, L. M. Smith, and S. N. Stechmann. Energy decompositions for moist Boussinesq and anelastic equations with phase changes. *Journal of the Atmospheric Sciences*, 76(11):3569–3587, 2019.
- [5] L. M. Smith and S. N. Stechmann. Precipitating quasigeostrophic equations and potential vorticity inversion with phase changes. J. Atmos. Sci., 74(10):3285–3303, 2017.
- [6] A. N. Wetzel, L. M. Smith, S. N. Stechmann, J. E. Martin, and Y. Zhang. Potential vorticity and balanced and unbalanced moisture. J. Atmos. Sci., 77(6):1913–1931, 2020.

## Progress in the analytical and numerical studies of the Hibler model of sea-ice dynamics

BOUALEM KHOUIDER (joint work with Clint Seinin, Sofiane Chatta, Salim Bensasi, Tahar Boulmezaoud)

#### 1. Introduction

Sea ice dynamics has long been recognized as a critical component of the Earth's climate system, influencing global temperatures, ocean circulation, and atmospheric patterns. Variations in sea ice extent are closely linked to climate change, acting both as indicators and amplifiers of global warming. Numerical models are used to capture sea-ice dynamics, predict its changes and understand their interactions with the broader climate system.

The first comprehensive model for sea-ice flourished from the Arctic Ice Dvnamics Joint Experiment (AIDJEX), where an elastic-plastic model for the ice displacement and deformation is coupled to an integro-differential equation for ice-thickness distribution [4], though with an open-ended plasticity yield curve. However, due to its complexity the AIDJEX model was replaced by a simpler version consisting of viscous-plastic equations for the momentum coupled to conservation equations for ice thickness and ice area-coverage (or concentration) based on an elliptic rheology [6]. Unfortunately, Hibler's system is severely stiff and analytically intractable. Many regularized versions have been proposed for both analytical studies and for numerical implementation, especially due to the abrupt transition between the viscous and plastic flow regimes. Some state-of-the-art climate models use the elasto-viscous-plastic (EVP) version due to [7], where the plastic deformation tensor is relaxed in time. But the EVP model introduces undesired artificial elastic waves leading to practical inaccuracies. An appealing alternative, consists in using a hyperbolic tangent to smoothen the viscous-plastic transition [8, 10].

In this talk, new analytic results showing that the regularized Hibler equations are linearly well posed, in both 1d and 2d [2, 3], and progress in using efficient and accurate numerical scheme for these equations are reported [10]. The performance of Crank-Nicholson and Backward differentiation-type schemes is also demonstrated. Further, for efficiently solving the original elastic-plastic equations for arbitrary yields is proposed [1].

#### 2. Highlights

AIDJEX (https://nsidc.org/data/aidjex) is the first comprehensive field campaign aimed at understanding sea-ice dynamics. The main result [4] of this experiment was to suggest based on observational evidence that at large scale, sea-ice dynamics can be modelled as an elasto-plastic material such as sands, gravels, clays, and fragmented rocks while the highly variable ice-thickness, due to the abundance of leads and ridges, can be modelled through a thickness distribution function

which obeys a continuum Smoluchowski-like kinetic equation. The coupled sea-ice momentum and ice-thickness equations take the form

(1) 
$$\frac{d\mathbf{v}}{dt} := \frac{D\mathbf{v}}{Dt} = -mf_c\mathbf{k} \times \mathbf{v} + \tau_w + \nabla \cdot \boldsymbol{\sigma} + \tau_a - m\hat{g}\nabla\phi.$$

(2) 
$$\frac{\partial G}{\partial t} + \mathbf{v} \cdot \nabla G := \frac{DG}{Dt} = -f \frac{\partial G}{\partial h} + (W - G)\nabla \cdot \mathbf{v},$$

where  $\mathbf{v}$  is the ice velocity field and  $G(h,t,R) = \frac{1}{|R|} \int_{\mathbf{x} \in R} H(h - \xi(\mathbf{x},t)) \, da$  is defined as the fractional area of ice thinner than h in a given ice-covered region R at time t, and  $\xi(x,t)$  is the actual-randomly varying ice thickness. Here, m if the mass density per unit area,  $f_c$  is the Coriolis parameter,  $\tau_w$  and  $\tau_a$  are the ocean and atmospheric stresses,  $\sigma$  is the vertically integrated internal ice stress,  $\hat{g}$  is the gravity acceleration and  $\phi$  is the surface geo-potential while f is the rate of melting and freezing and W is the ice ridging and opening function.

The tensor  $\sigma$  is given in terms of the strain tensor  $\dot{\epsilon} = \frac{1}{2}(\nabla v + \nabla v^T)$  and a messure of ice strength  $p^*$ , via Hooke's law when the ice-flow is elastic and through a normal-plastic flow rule during the elastic regime, when the maximum yield is reached:  $F(\sigma, p^*) = 0$ ;  $p^*$  is related to the G(h) through an energy balance relation. While the field work didn't allow a definitive yield curve F, a few suggestions have been made. It is for instance suggested that because sea-ice has zero resistance to tensile stress, the yield curve should be contained in the third quadrant in the plane of principle stresses (eigenvalues of  $\sigma$ ).

Hibler's model [6] was suggested as a mathematically and numerically accessible simplification of the AIDJEX model. It consists of an elliptic yield curve and a coarse thickness distribution reduced to two ice categories: thin ice and thick ice. The elliptic curve in particular allowed a closed form inversion of the plastic flow rule:

$$\sigma = \frac{\xi - \eta}{2} \operatorname{tr}(\dot{\epsilon}) + \eta \dot{\epsilon} - \frac{p^*}{2} I_d, \ \xi = \frac{p^*}{\max(\Delta, \Delta_0)}, \ \eta = \frac{\xi}{e^2}, \ \Delta = \sqrt{\dot{\epsilon}_I^2 + \frac{1}{e} \dot{\epsilon}_{II}^2}.$$

Here,  $\xi$  and  $\eta$  are the bulk and shear viscosities while  $\dot{\epsilon}_I$  and  $\dot{\epsilon}_{II}$  are the normal and shear strains, respectively and e the ellipticity constant. The max cutt-off in the expression of  $\xi$  is to avoid singular behaviour when the strain is zero and further simplifies the model into a viscous-plastic system, avoiding carying through the elastic regime which is deemed negligible. This cutt-off however led to another challenge. The equations became numerically stiff and analytically intractable. To improve the numerics, Lemieux et al. [8] introduced the tanh regularization:

(3) 
$$\xi = KP \tanh\left(\frac{1}{2K\Delta}\right),$$

where K is a (large) dimensional constant, and suggested a Jacobian-free-Newton-Krylov (JFNK) solver for the regularized Hibler sea-ice momentum equations, which showed a lot of promise. An improved version of the JFNK solver and a validation against a synthetic solution is done in [10]. The improvement had many levels including the use of second order time integration via a Crank-Nicholson

(CN) scheme, instead of the backward Euler used in [8], and a better approximation of Jacobian-vector multiplication using a second order approximation of the Gateaux derivative. Numerical tests showed an overall second order convergence in both time and space and a faster convergence of the Newton solver, less than 10 iterations compared to 50 to 100 used in the previous works. Furthermore, the superiority of the CN scheme compared to the backward Euler was demonstrated.

In terms of analysis, previous work showed that Hilber's model is linearly ill posed in 1d while in 2d existing results are inconclusive. In [2], it is shown that in 1d, the tanh-regularized Hibler equations are linearly well posed, uniformly, for all flow configurations while in [3], linear well-posedness for the same model is obtained for the linear model with frozen coefficients, when the flow gradient is finite. For infinite flow gradients (e.g. infinite convergence/divergence or shear), the well-posedness of the linear system is inconclusive in some regimes; the parabolicity of the system can be lost when the flow-gradient is infinite and the equations become numerically ill conditioned. The numerical inversion becomes highly inaccurate and the time integration becomes stiff.

Nonetheless, rigorous well-posedness results have been obtained for other forms of regularized and modified Hibler's model of sea ice [5, 9].

A new way of handling the original elastic-plastic model of sea ice, with any convex yield curve, is suggested in [1], using convex analysis. The main idea was to project the elasto-plastic equations onto the tangent and normal cones of the yield curve, in the manifold of symmetric tensors, consistently with the normal flow rule. The main result is an evolution equation for the stress tensor:

(4) 
$$\dot{\sigma} = \mathbb{H}(\dot{\epsilon}) - \mathbb{H}\left(\Pi_{(N(C(p^*),\sigma)}\left(\dot{\epsilon} - \frac{\dot{p^*}}{p^*}\mathcal{H}^{-1}(\sigma)\right)\right),$$

where  $\Pi_{(N(C(p^*),\sigma)}$  is the projection onto the normal cone of the yield curve  $C(p^*)$  at  $\sigma$ . Such projections for many yield curve prototypes, with and without singularities, have been readily obtained [1]. This equation can thus be solved in together with the equations in (1) and (2) without the need for the inversion of the flow rule. The numerical implementation for the elliptic yield curve of Hibler and many others that have not yet been tested such as Tresca and Mohr-Coulomb will be considered in future work.

- [1] BOULMEZAOUD, T. Z., KHOUIDER, B.: A new mathematical formulation of the equations of perfect elasto-plasticity, Zeitschrift für angewandte Mathematik und Physik, 73, 246 (2022).
- [2] Soufiane Chatta, Boualem Khouider, M'hamed Kesri; Linear well posedness of regularized equations of sea-ice dynamics. J. Math. Phys. 1 May 2023; 64 (5): 051504. https://doi.org/10.1063/5.0152991
- [3] Soufiane Chatta and Boualem Khouider; Linear well posedness of the regularized-Hibler model of sea-ice dynamics in 2d. *Manuscript*. Submitted to Journal of Nonlinear Science.
- [4] M. Coon, M., Maykut, G., Pritchard, R., Rothrock, D., Thorndlike, A.: Modeling the pack ice as an elastic-plastic material, AIDJEX Bulletin, vol. 24 (1974).
- [5] Felix Brandt, Karoline Disser, Robert Haller-Dintelmann, and Matthias Hieber. Rigorous analysis and dynamics of Hibler's sea ice model. J. Nonlinear Sci., 32:50, 2022.

- [6] HIBLER III, W.: A dynamic thermodynamic sea ice model, Journal of Physical Oceanography, Vol. 9 (1979), pp. 815–846.
- [7] E. C. Hunke, "Viscous-plastic sea ice dynamics with the EVP model: Linearization issues,"
   J. Comput. Phys. 170(1), 18–38 (2001). https://doi.org/10.1006/jcph.2001.6710
- [8] J.-F. Lemieux and B. Tremblay, "Numerical convergence of viscous-plastic sea ice models,"
   J. Geophys. Res. 114(C5), 1–14, (2009). https://doi.org/10.1029/2008jc005017
- [9] Xin Liu, Marita Thomas, and Edriss S. Titi. Well-posedness of Hibler's dynamical sea-ice model. J. Nonlinear Sci., 32:49, 2022.
- [10] C. Seinen and B. Khouider, "Improving the Jacobian free Newton-Krylov method for the viscous-plastic sea ice momentum equation." Physica D 376, 78–93 (2018).

# The primitive equations subject to deterministic and stochastic forces Matthias Hieber

(joint work with A. Agresti, T. Binz, F. Brandt, A. Hussein, M. Saal, T. Zöchling)

In this talk we study first the primitive equations with non-isothermal turbulent pressure and transport noise. They are derived from the Navier-Stokes equations by employing stochastic versions of the Boussinesq and hydrostatic approximations. For such a model we prove global well-posedness in  $H^1$ , where the noise is considered in both the Ito and Stratonovich formulations. The proof is based on stochastic maximal regularity estimates.

Secondly, we investigate the primitive equations under the influence of stochastic wind driven boundary conditions modeled by a cylindrical Wiener process. A combination of deterministic and stochastic methods yield that these equations admit a unique, local pathwise solution within the anisotropic  $L_t^p - H_z^{-1,p} L_{xy}^p$ -setting. Moreover, the solution is constructed in critical spaces.

Finally, we combine the above two results to investigate a coupled atmosphereocean model due to Lions, Temam and Wang. It concerns a system of two fluids described by two primitive equations coupled by fully nonlinear interface conditions.

- [1] A. Agresti, M. Hieber, A. Hussein, M. Saal, The stochastic primitive equations with non-isothermal turbulent pressure, Ann. Appl. Prob. 35 (2025), 635–700.
- [2] T. Binz, M. Hieber, A. Hussein, M. Saal, The primitive equations with stochastic wind driven boundary conditions, J. Math. Pures Appl. 183 (2024), 76–101.
- [3] T. Binz, F. Brandt, M. Hieber, T. Zöchling, Global strong well-posedness of the CAOproblem introduced by Lions, Teman and Wang, arXiv:2505.11952.

## Well-posedness of a non-local Ocean-Atmosphere coupling model Sophie Thery

Interactions between the ocean and the atmosphere play an essential role in climate modelling and weather forecasting. Oceanic and atmospheric models have been built separately by two distinct communities and coupled via complex interface conditions. We propose to translate this coupled system into a global mathematical model in order to use the analysis tools and study its well-posedness. We present a simplified but realistic model containing the main ingredients of numerical models. This mathematical model is known as the coupled Ekman problem, taking into account the vertical exchanges of horizontal currents and the effect of small scales via turbulent viscosities. The special feature of this model is that it considers the interface as a buffer zone between the two domains, with interface conditions specific to the ocean-atmosphere coupling. These interface conditions lead to the dependence of viscosity profiles on the trace of solutions around the interface and make the global problem non-local.

To study the well-posedness of this system, a first method consists of rewriting it as a fixed-point problem in order to deal with the non-local aspects. This strategy is inspired by work [1] which considers a model with same kind of non local behavior. A general study of the problem in its stationary and non-stationary states leads to a sufficient condition to guarantee the uniqueness of the solutions. This condition, applied to the ocean-atmosphere framework, i.e. with physically realistic viscosity conditions, makes it possible to obtain a good resolution of the problem. This condition applied to the ocean-atmosphere framework, i.e. with viscosity profiles find in litterature for ocean and atmosphere application and orders of magnitude, is too restrictive and does not guarantee the uniqueness of the solutions. In the stationary case, a necessary and sufficient condition can be given to ensure the existence and uniqueness of solutions. We will see that, once again, in the context of ocean-atmosphere coupling, this condition is not met and there is no uniqueness of solutions. In conclusion, we discuss the prospects for such a model and the parameters that could be adjusted to obtain a mathematically wellposed model. In particular, we point out the role of interface parameterisation and the inconsistency between the numerical constraints and the physical constraints acting on this parameterisation. The presented results are detailled in [2].

Discussions after this presentation highlighted possibilities for improvement. First, more complex viscosity profiles need to be taken into account to reflect the reality of the Ocean-Atmosphere models, especially in the unsteady state. That said, even if our model is simplified, the criteria that we establish contain the same ingredients and follow the same behavior as in [1] which consider more complex viscosity profiles. It seems that it is the order of magnitude described by the ocean-atmosphere framework that does not fall within the scope of this method. Another point highlighted was the problem of testing the results, as there is no simplified model that can be used as a test case for the results presented here. As the model is a simplified version of the ocean-atmosphere model, it is of course difficult to draw direct conclusions about realistic numerical models, but it does

highlight the elements that could break the mathematical consistency of these models.

#### References

- [1] C. Bernardi, T. Chacón Rebollo, R. Lewandowski, and F. Murat, A model for two coupled turbulent fluids. part i: analysis of the system, Studies in Mathematics and its Applications 31 (2002), 69–102
- [2] S. Thery, Well-posedness of a non local ocean-atmosphere coupling model: study of a 1D Ekman boundary layer problem with nonlocal KPP-type turbulent viscosity profile, Annales Mathematiques Blaise Pascal, accepted (2025)

## Scaling regimes for moist atmospheric flows and the Clausius-Clapeyron relation

Daniel Bäumer

(joint work with Rupert Klein, Norbert J. Mauser)

In the early 2000s, Rupert Klein proposed a general framework for understanding model hierarchies in the fluid dynamics of the earth's atmosphere. This framework, comprehensively described in [1], was built on the basis of a distinguished limit for the so-called universal characteristics of atmospheric motion, valid for dry air. Obtaining an extension of said distinguished limit that includes the thermodynamic parameters of moist, cloudy air would be of considerable theoretical and practical interest. In this talk, we learn about the difficulties arising in this endeavor from incorporation of the fundamental Clausius-Clapeyron relation for the saturation vapor pressure, and we present two contrasting approaches to their resolution, based on the discussion in [2].

#### References

- R. Klein, Scale-Dependent Models for Atmospheric Flows, Annu. Rev. Fluid Mech. 42 (2010), 249–274.
- D. Bäumer, R. Klein and N.J. Mauser, A general framework for the asymptotic analysis of moist atmospheric flows, submitted.

## Finite energy weak solutions to a multilayered 3D fluid-poroelastic structure interaction problem

FELIX BRANDT

(joint work with Sunčica Čanić, Boris Muha)

Fluid-poroelastic structure interaction (FPSI) problems have gained a lot of attention recently in numerical and mathematical analysis. This is also due to its broad applications in fields such as biomedical engineering, geomechanics and petroleum engineering, civil engineering, environmental engineering, aerospace and marine

engineering or energy systems. For the investigation of a linearly coupled 3D-"2.5D"-3D FPSI problem, we refer to [1]. The nonlinearly coupled case of a 2D-1D-2D model has been addressed in [3].

In this talk, we discuss the existence of a finite energy weak solution to a nonlinearly coupled multilayered 3D FPSI problem. At the top, we consider a thick poroelastic Biot model, which is separated from the incompressible, viscous fluid by a thin reticular plate. The latter acts as a moving interface with mass between the two thick layers. The model is complemented by suitable kinematic coupling conditions, including the Beavers-Joseph-Saffman conditions for tangential slip, and dynamic coupling conditions.

The existence of a finite energy weak solution to a regularized version of the model is obtained by means of semidiscretization and a splitting scheme. The lack of Lipschitz regularity of the fluid domain poses significant challenges when establishing weak and weak\* convergences of subsequences of the sequence of approximate solutions. The upgrade to strong convergence for the limit passage in the nonlinear problem involves compactness results due to Dreher and Jüngel [2] for piecewise constant functions as well as a generalized Aubin-Lions compactness criterion for moving domains [4].

#### References

- L. Bociu, S. Čanić, B. Muha, J.T. Webster. Multilayered poroelasticity interacting with Stokes flow. SIAM J. Math. Anal. 53 (2021), 6243–6279.
- [2] M. Dreher, A. Jüngel. Compact families of piecewise constant functions in  $L^p(0, T; B)$ . Nonlinear Anal. **75** (2012), 3072–3077.
- [3] J. Kuan, S. Čanić, B. Muha. Fluid-poroviscoelastic structure interaction problem with non-linear geometric coupling. J. Math. Pures Appl. (9) 188 (2024), 345–445.
- [4] B. Muha, S. Čanić. A generalization of the Aubin-Lions-Simon compactness lemma for problems on moving domains. J. Differential Equations 266 (2019), 8370–8418.

## Mixing Estimates for Passive Scalar Transport by Sobolev and BVVector Fields

#### Lucas Huysmans

We study the rate at which small scale structures, or 'mixing', emerges in incompressible fluids. We consider the linear passive scalar transport equation with a divergence-free, vector field u(x,t). Denoting the transported passive scalar field by  $\rho(x,t)$ , we arrive at the classical transport partial differential equation:

$$\frac{\partial \rho}{\partial t}(x,t) + u(x,t) \cdot \nabla \rho(x,t) = 0.$$

In the mathematical literature one usually measures such mixing by the decay of negative Sobolev norms, such as  $W_x^{-1,1}$ , which measure the average length scale present in the passive scalar [2]. One expects that the size of such length scales are

bounded (from below) by an exponential in the time variable and the regularity of the vector field. For instance in [5], using estimates from [7], it was proved that

$$\|\rho(\cdot,T)\|_{W_x^{-1,1}} \ge A(\rho_0) \exp\left(-C(\rho_0) \int_0^T \|\nabla u(\cdot,t)\|_{L_x^p} dt\right),$$

where  $A(\rho_0), C(\rho_0) > 0$  are constants depending on the initial datum  $\rho_0(x) = \rho(x,0)$ . We improve on these results, using estimates from [6] to give in [9] new expressions for these constants, with in particular  $C(\rho_0)$  given by

$$C(\rho_0) = C_p \frac{\|\rho_0\|_{L_x^{\frac{p}{p-1}}}}{\|\rho_0\|_{L_x^{\frac{1}{p}}}},$$

which has the correct units of length to the power  $-\frac{d}{p}$  (with d the dimension) to ensure the exponent in the mixing rate is dimensionless. However, the constant  $C_p$  blows up as  $p \to 1$ . Finding any quantitative mixing rate in the case p = 1 remains an important open problem, despite well-posedness in this class [3], [1], and is the subject of a famous open conjecture by Bressan [8].

In this direction, we give in [4] the first bound in terms of the  $W_x^{1,1}$  norm of  $\nabla u(x,t)$ , or more generally the  $BV_x$  norm of u(x):

$$\|\rho(\cdot,T)\|_{W_x^{-1,1}} \ge \left(e^{e^{e^{\cdot\cdot\cdot^e}}}\right)^{-1}$$

where

$$N = A(\rho_0) \exp \left( C(\rho_0) \int_0^T \|\nabla u(\cdot,t)\|_{L^1_x} \ dt \right),$$

for some constants  $A(\rho_0), C(\rho_0) > 0$ .

- L. Ambrosio. Transport equation and Cauchy problem for BV vector fields. Invent. Math., 158(2):227-260, 2004. ISSN 0020-9910,1432-1297. URL https://doi.org/10.1007/s00222-004-0367-2.
- [2] G. Alberti, G. Crippa, and A. L. Mazzucato. Exponential self-similar mixing by incompressible flows. J. Amer. Math. Soc., 32(2):445–490, 2019. ISSN 0894-0347,1088-6834. URL https://doi.org/10.1090/jams/913.
- [3] R. J. DiPerna and P.-L. Lions. Ordinary differential equations, transport theory and Sobolev spaces. *Invent. Math.*, 98(3):511-547, 1989. ISSN 0020-9910. URL https://doi.org/10.1007/BF01393835.
- [4] L. Huysmans and A. R. Said. Mixing Estimates for Passive Scalar Transport by BV Vector Fields. arXiv preprint arXiv:2504.03023, 2025.
- [5] G. Iyer, A. Kiselev, and X. Xu. Lower bounds on the mix norm of passive scalars advected by incompressible enstrophy-constrained flows. *Nonlinearity*, 27(5):973–985, 2014. ISSN 0951-7715,1361-6544. URL https://doi.org/10.1088/0951-7715/27/5/973.
- [6] M. Hadžić, A. Seeger, C. K. Smart, and B. Street. Singular integrals and a problem on mixing flows. Ann. Inst. H. Poincaré C Anal. Non Linéaire, 27(4):921-943, 2018. ISSN 0294-1449,1873-1430. URL https://doi.org/10.1016/j.anihpc.2017.09.001.

- [7] G. Crippa and C. De Lellis. Estimates and regularity results for the DiPerna-Lions flow. J. Reine Angew. Math., 616:15-46, 2008. ISSN 0075-4102,1435-5345. URL https://doi.org/10.1515/CRELLE.2008.016.
- [8] A. Bressan. A lemma and a conjecture on the cost of rearrangements. Rend. Sem. Mat. Univ. Padova, 110:97–102, 2003. ISSN 0041-8994.
- [9] L. Huysmans and A. R. Said. Quantitative Estimates in Passive Scalar Transport: A Unified Approach in W<sup>1,p</sup> via Christ-Journé Commutator Estimates. arXiv preprint arXiv:2402.11642, 2025.

### Advection by turbulent velocity fields

László Székelyhidi Jr.

(joint work with Jan Burczak and Bian Wu)

A fundamental concept in turbulence is the idea of an energy cascade. Introduced by Richardson in 1926, it refers to a self-similar process whereby energy is continuously transferred to higher (or lower) wavenumbers, resulting in a forward (or backward) cascade. Assuming such a self-similar mechanism to exist and is complemented by a continuous input of energy at one end of the spectrum and a continuous loss of energy at the other end of the spectrum, one is formally lead to the concept of enhanced or anomalous dissipation.

Whilst the nature of the energy cascade in the Navier-Stokes system remains elusive, considerable progress has been made on the analogous scalar problem. Here one considers the transport-diffusion equation

$$\partial_t \rho + u \cdot \nabla \rho = \kappa \Delta \rho,$$

in a spatial domain  $\Omega$ , which in the simplest settings would be a periodic box  $\mathbb{T}^2$  or  $\mathbb{T}^3$  and complemented with an initial condition  $\rho(x,0) = \rho_{in}(x)$ . For simplicity we assume that the scalar  $\rho$  has vanishing spatial average,  $\int \rho \, dx = \int \rho_{in} \, dx = 0$ . Under very mild conditions on the velocity field there exists a unique global-in-time solution. The energy identity reads

$$\frac{1}{2}\frac{d}{dt}\int_{\Omega} |\rho(x,t)|^2 dx = -\kappa \int_{\Omega} |\nabla \rho(x,t)|^2 dx.$$

Using the Poincaré inequality we deduce the energy decay bound

$$\int_{\Omega} |\rho(x,t)|^2 dx \le C e^{-\kappa \ell_0^{-2} t} \int_{\Omega} |\rho_{in}(x)|^2 dx,$$

where  $\ell_0$  can be interpreted as the length-scale of the domain  $\Omega$ . However, this bound is ignorant of the possible effect of advection by the velocity field u - for instance, assuming that advection by u induces a transfer of the initial  $L^2$ -energy of  $\rho$  in Fourier space to higher wavenumbers at length-scale, say,  $\ell \ll \ell_0$ , we could heuristically expect to replace  $\ell_0$  in the above decay bound by  $\ell$ , leading to faster decay for the same value of  $\kappa$  (equivalently, the same decay rate at smaller  $\kappa$ ). A more formal way of saying this is to estimate the "diffusion time" associated to the advection diffusion equation, that is the time it takes for the  $L^2$  norm to reduce by a fixed factor. The above estimate would lead to a diffusion time of

the order  $T_{diff} \sim \kappa^{-1}$ , which is precise for the heat equation without advection. Assuming, as above, that advection induces a self-similar process (a cascade) of the  $L^2$  norm of  $\rho$  to move to larger and larger wavenumbers can, in principle, lead to faster diffusion. If  $T_{diff} \sim \kappa^{-\alpha}$  for some  $\alpha < 1$ , one speaks of "enhanced diffusion"; if  $T_{diff} \sim 1$  (i.e. independent of  $\kappa$ ), one speaks of anomalous diffusion. The heuristics of anomalous diffusion and its relation to a cascade mechanism have been analysed in numerous works, in the talk we presented the heuristic arguments of E. Lorenz [1] as well as Obukhov-Corrsin [2]-[3]. In particular it is easy to see by a simple scaling analysis that  $C^{1,\alpha}$  vector fields may lead to enhanced but not anomalous dissipation, whereas  $C^{\alpha}$  vector fields may lead to anomalous dissipation, for any  $\alpha < 1$ . The latter is of course relevant for the context of 3D turbulence: as anticipated by Onsager [4], velocity fields in fully developed turbulent flows away from boundaries are expected to behave like Hölder continuous vectorfields with exponent  $\alpha \sim 1/3$ .

These heuristics have rigorous mathematical analogues. In the PDE literature Onsager's conjecture was resolved for physically meaningful weak solutions of the Euler equations

$$\partial_t u + u \cdot \nabla u + \nabla p = 0,$$
  
$$\operatorname{div} u = 0.$$

i.e. those for which kinetic energy monotonically decreases, in [5]: for any  $\alpha < 1/3$  there exists weak solutions u = u(x,t) on  $\mathbb{T}^3 \times [0,T]$ , for which the kinetic energy is strictly decreasing. The exponent 1/3 is optimal [9].

The issue of anomalous scalar dissipation has first been raised in [6], where an example of anomalous dissipating flow was given. This was followed by several other constructions, notably [7, 8]. The velocity field and the scalar are both Hölder continuous, with exponent  $\alpha, \beta < 1$ , respectively, with  $\alpha + 2\beta < 1$ , the range in agreement with the Obukhov-Corrsin scaling theory. The precise statement is as follows: there exists  $T_* > 0$  and  $c_* > 0$  such that for any sufficiently regular initial data  $\rho_{in}$  the unique solution  $\rho_{\kappa}$  of the transport-diffusion equation satisfies

$$\liminf_{\kappa \to 0} \kappa \int_0^{T_*} \int_{\Omega} |\nabla \rho_{\kappa}|^2 dx dt \ge c_*.$$

This is equivalent to saying that the diffusion time  $T_{diff} \sim T_*$  is independent of  $\kappa \to 0$ .

The basic mechanism leading to anomalous dissipation, which is the key point in the constructions above, is mixing: strong mixing properties of the velocity field are responsible for the cascade process described above. In a nutshell, mixing in the context of refers to the (quantitative) decay of the negative Sobolev norm  $\|\rho(t)\|_{H^{-1}}$ , which, taking the interpolation inequality  $\|\rho\|_{L^2} \leq C\|\rho\|_{H^{-1}}^{1/2}\|\rho\|_{H^1}^{1/2}$  as heuristic, can be related to growth of  $H^1$  norm, possibly leading to an enhanced diffusion rate. We refer to [10] for the relationship between mixing and enhanced dissipation. The examples [6, 7, 8] have a common feature in that anomalous dissipation occurs at a single time  $T_*$ . At this time the velocity field stops being smooth. In fact, there is a sequence of times  $T_k < T_{k+1} < \cdots \rightarrow T_*$  such that in

each time interval the vector field mixes at finer and finer scales, in a self-similar fashion. Thus, the cascade referred to above is a process happening "dynamically" in time. On the other hand, the energy cascade in the context of turbulence is a statistically stationary process, where anomalous dissipation is expected to occur at every time. This can be seen in the following consequence of the fluctuation-dissipation relation, derived in the setting of the (deterministic) transport-diffusion equation as above in [11]:

$$\kappa \int_0^T \int_{\Omega} |\nabla \rho_{\kappa}|^2 dx dt \sim \int_{\Omega} \mathbb{E}^{1,2} |X_T^{(1)} - X_T^{(2)}|^2 dx$$

for appropriate (random) initial datum  $\rho_{in}$ , where  $X_t^{(i)}$ , i=1,2 are two independent copies of the (random) Lagrangian flow map. In the turbulence literature the time evolution of the relative distance of two tracer particles is referred to as pair dispersion. The basic scaling law, due to Richardson 1926, states  $|X_T^{(1)} - X_T^{(2)}|^2 \sim T^{2/3}$  in an appropriate range of space and time.

In recent work [13], based on the technique of iterative homogenization in the context of transport-diffusion equation pioneered by S. Armstrong and V. Vicol in [12], we show that typical  $C^{\alpha}$ ,  $\alpha < 1/3$ , weak solutions of the 3D Euler equations u lead to anomalous dissipation for the transport-diffusion equation in the form

$$\limsup_{\kappa \to 0} \kappa \int_0^T \int_{\Omega} |\nabla \rho_{\kappa}|^2 \, dx \, dt \ge c_* T^{\frac{2}{1-\alpha}} \left(\frac{\ell_{in}}{\ell_0}\right)^{\frac{1+\alpha}{1-\alpha}} \ell_0^{-2} \|\rho_{in}\|_{L^2}^2,$$

where  $\ell_{in} = \frac{\|\rho_{in}\|_{L^2}}{\|\nabla\rho_{in}\|_{L^2}}$  is a length scale associated with the initial data. Thus, here the cascade takes place at every time, and in the limit  $\alpha \to 1/3$  we recover the Richardson law "on average". In the talk we discuss the basic idea of the proof and comment on possible extensions as well as limitations of the approach.

- [1] E. Lorenz, The predictability of a flow which possesses many scales of motion, Tellus 21 (1969), 289–307.
- [2] A. M. Obukhov, Structure of temperature field in turbulent flow, Izv. Akad. Nauk. SSSR, Geogr. Geofiz, 13 1949.
- [3] S. Corrsin, On the spectrum of isotropic temperature fluctuations in an isotropic turbulence,
   J. Appl. Phys. 22 (1951), 469–473.
- [4] L. Onsager, Statistical hydrodynamics, Nuovo Cimento (9) 6 (1949), Supplemento, no. 2 (Convegno Internazionale di Meccanica Statistica), 279–287.
- [5] T. Buckmaster et al., Onsager's conjecture for admissible weak solutions, Comm. Pure Appl. Math. 72 (2019), no. 2, 229–274.
- [6] T. D. Drivas et al., Anomalous dissipation in passive scalar transport, Arch. Ration. Mech. Anal. 243 (2022), no. 3, 1151–1180.
- [7] M. Colombo, G. Crippa and M. Sorella, Anomalous dissipation and lack of selection in the Obukhov-Corrsin theory of scalar turbulence, Ann. PDE 9 (2023), no. 2, Paper No. 21.
- [8] T. M. Elgindi and K. Liss, Norm growth, non-uniqueness, and anomalous dissipation in passive scalars, Arch. Ration. Mech. Anal. 248 (2024), no. 6, Paper No. 120.
- [9] P. Constantin, W. E and E. S. Titi, Onsager's conjecture on the energy conservation for solutions of Euler's equation, Comm. Math. Phys. 165 (1994), no. 1, 207–209.

- [10] M. Coti Zelati, M. G. Delgadino and T. M. Elgindi, On the relation between enhanced dissipation timescales and mixing rates, CPAM 73 (2020), no. 6, 1205–1244.
- [11] T. D. Drivas and G. L. Eyink, A Lagrangian fluctuation-dissipation relation for scalar turbulence. Part I. Flows with no bounding walls, J. Fluid Mech. 829 (2017), 153–189.
- [12] S. N. Armstrong and V. C. Vicol, Anomalous diffusion by fractal homogenization, Ann. PDE 11 (2025), no. 1, Paper No. 2, 145 pp.
- [13] J. Burczak, L. Székelyhidi Jr. and B. Wu, Anomalous dissipation and Euler flows, arXiv (2024), https://arxiv.org/abs/2310.02934.

## Numerical aspects of simulating large-scale sea-ice dynamics CAROLIN MEHLMANN

This talk addresses recent advances in the numerical modeling of viscous-plastic sea-ice dynamics. Starting from the classical Hibler-type sea-ice model [1], we derive a formulation suitable for numerical analysis and the application of modern approximation techniques. We then present a novel finite element method developed for use in climate models such as ICON [3].

### GOVERNING EQUATIONS

In most current climate models, sea ice is treated as a two-dimensional viscousplastic material [1]. The sea-ice motion is described by three variables: sea-ice concentration  $A(x,t) \in [0,1]$  (the fraction of a grid cell covered with ice), mean ice thickness  $h(x,t) \in [0,\infty)$ , and sea-ice velocity  $\mathbf{v}(x,t) \in \mathbb{R}^2$ . The concentration and thickness evolve over time via transport equations, while the velocity is determined from the momentum equation:

(1) 
$$\rho h \partial_t \mathbf{v} = \mathbf{F}_{\text{ext}} + \text{div}(\boldsymbol{\sigma}),$$

where  $\rho$  is the sea-ice density and  $\mathbf{F}_{\rm ext}$  collects the external forces, including wind stress, ocean drag, and the Coriolis force. The viscous-plastic rheology defines the relation between internal stress  $\boldsymbol{\sigma}$  and the strain rates:

(2) 
$$\frac{1}{2}(\nabla \mathbf{v} + \nabla \mathbf{v}^T) =: \dot{\boldsymbol{\epsilon}} = \dot{\boldsymbol{\epsilon}}' + \frac{1}{2}\operatorname{tr}(\dot{\boldsymbol{\epsilon}})I.$$

We introduce the rheology in terms of the trace and deviatoric parts of the strain rate tensor [5]:

$$\boldsymbol{\sigma} := \frac{1}{2} \zeta \dot{\boldsymbol{\epsilon}}'(\mathbf{v}) + \zeta \operatorname{tr}(\dot{\boldsymbol{\epsilon}}(\mathbf{v})) I - \frac{P}{2} I,$$

where the viscosity  $\zeta$  and the ice strength P are given by:

$$\zeta := \frac{P}{2 \max(\Delta_P(\mathbf{v}), \Delta_{\min})}, \qquad P := H \exp(20(1 - A)),$$
  
$$\Delta_P(\mathbf{v}) := \frac{1}{2} \dot{\boldsymbol{\epsilon}}' : \dot{\boldsymbol{\epsilon}}' + \operatorname{tr}(\dot{\boldsymbol{\epsilon}})^2, \qquad \Delta_{\min} = 2 \times 10^{-9}.$$

To ensure a smooth transition between the viscous closure,  $\Delta_{\min}$ , and plastic regimes,  $\Delta_P(\mathbf{v})$ , we follow [2] and define the regularized strain rate invariant:

(3) 
$$\Delta(\dot{\epsilon}) = \sqrt{\Delta_P(\dot{\epsilon})^2 + \Delta_{\min}^2}.$$

This regularization enables the simulation of both viscous stresses and plastic stresses [5]. We write the weak form of the stress tensor as:

(4) 
$$(\boldsymbol{\sigma}, \nabla \phi) = 2(\zeta \boldsymbol{\tau}(\dot{\boldsymbol{\epsilon}}), \boldsymbol{\tau}(\boldsymbol{\phi})) + \left(\frac{P}{2}, \operatorname{tr}(\dot{\boldsymbol{\epsilon}}(\boldsymbol{\phi}))\right)$$
$$= \mathcal{A}(\mathbf{v})(\boldsymbol{\phi}) + \left(\frac{P}{2}, \operatorname{tr}(\dot{\boldsymbol{\epsilon}}(\boldsymbol{\phi}))\right),$$

where  $\tau(\dot{\boldsymbol{\epsilon}}) := \frac{1}{2}\dot{\boldsymbol{\epsilon}}' + \frac{1}{2}\operatorname{tr}(\dot{\boldsymbol{\epsilon}})I$ . The operator  $\mathcal{A}(\mathbf{v})(\phi)$  has structural similarities with the regularized p-Laplacian and time-dependent minimal surface problems [5]. By exploiting the symmetric positive definite structure of the Jacobian [4], we show that the time-discretized problem defines a convex functional bounded from below [7]. This structure enables the design of efficient Newton solvers for finite element and finite difference settings [4, 5, 7].

#### SPATIAL DISCRETIZATION AND ERROR ANALYSIS

To discretize the sea-ice momentum equation on a spherical geometry (e.g. the Earth), I introduced a nonconforming vector-valued finite element: the surface Crouzeix–Raviart (sCR) element [6]. This element places degrees of freedom at the edge midpoints, which aligns well with ocean models using similar staggering (e.g., ICON-O [3]).

We consider a triangulated surface  $\Gamma_h$  approximating a smooth, closed surface  $\Gamma \subset \mathbb{R}^3$ , where the vertices of the  $\Gamma_h$  coincide with  $\Gamma$ . The discrete sCR element space on  $\Gamma_h$  is given by

$$V_h^{ an} = \left\{ \mathbf{v} : \Gamma_h \to \mathbb{R}^3 \,\middle|\, \mathbf{v}|_K \in V_K, \text{ continuous vector components at } m_E \right\},$$

where  $m_E$  denotes the edge midpoint of triangle  $K \in \Gamma_h$ , and  $V_K$  is spanned by tangential and normal components of locally planar basis functions. A detailed description of the finite element space is given in [8]. Approximating the surface Laplacian problem with the sCR element, I proved the following error estimates between the finite element solution  $\mathbf{u}_h$  on  $\Gamma_h$  and the extended exact solution  $\mathbf{u}_e$  from  $\Gamma$  to  $\Gamma_h$ :

(5) 
$$\|\mathbf{u}_e - \mathbf{u}_h\|_h \le ch \|\mathbf{f}\|_{L^2(\Gamma)},$$

(6) 
$$||P(\mathbf{u}_e - \mathbf{u}_h)||_{L^2(\Gamma_h)} \le ch^2 ||\mathbf{f}||_{L^2(\Gamma)},$$

where P denotes the orthogonal projection and  $\|\cdot\|_h$  is a discrete energy norm. The proof is given in [8].

These theoretical results are confirmed by numerical experiments conducted in the framework of the climate model ICON [3]. Let x, y, z denote Cartesian coordinates, and R is the Earth's radius. We solve

(7) 
$$-\operatorname{div}_{\Gamma}\left(\frac{\zeta}{2}\nabla_{\Gamma}\mathbf{v}\right) + \frac{1}{100}\mathbf{v} = \mathbf{f},$$

where  $\operatorname{div}_{\Gamma}$  and  $\nabla_{\Gamma}$  are the surface divergence and gradient, respectively. The viscosity,  $\zeta$ , the forcing,  $\mathbf{f}$  and the analytic solution  $\mathbf{v}^*$  are given by:

$$\zeta = 2.75 \cdot 10^{13}, \quad \mathbf{f} = -\text{div}_{\Gamma} \left( \frac{\zeta}{2} \nabla_{\Gamma} \mathbf{v}^* \right) + \frac{1}{100} \mathbf{v}^*, \quad \mathbf{v}^* = \left( \sin(10^{-6} Ry), 0, 0 \right).$$

We discretize the sphere with triangles of edge lengths 316 km, 158 km, and 79 km. The  $H^1$ -error and  $L^2$ -error between exact and numerical solutions are reported in Table 1, showing first- and second-order convergence, respectively, consistent with (5) and (6). A detailed discussion is given in [8].

Table 1. Error evaluation for (7) discretized with vector-valued surface Crouzeix–Raviart elements.

Mesh size	$L^2$ -error	Order	$H^1$ -error	Order
	$1.6880 \cdot 10^{-2}$		$3.7166 \cdot 10^{-1}$	-
158  km	$4.2288 \cdot 10^{-3}$	2.00	$1.8613 \cdot 10^{-1}$	1.00
79  km	$1.0605 \cdot 10^{-3}$	2.00	$9.3103 \cdot 10^{-2}$	1.00

#### References

- W.D. Hibler, A dynamic thermodynamic sea ice model, J. Phys. Oceanogr., 9 (1979), 815– 846.
- M. Kreyscher et al., Evaluation of sea ice rheology schemes for use in climate simulations,
   J. Geophys. Res., 105 (2000), 299–320.
- [3] P. Korn, Formulation of an unstructured grid model for global ocean dynamics, J. Comput. Phys., 339 (2017), 525-552.
- [4] C. Mehlmann, T. Richter, A modified global Newton solver for viscous-plastic sea ice models, Ocean Model., 116 (2017), 96–107.
- [5] C. Mehlmann, Efficient numerical methods to solve the viscous-plastic sea ice model at high spatial resolutions, PhD Thesis (2019), doi:10.25673/14011.
- [6] C. Mehlmann, O. Gutjahr, Discretization of sea ice dynamics in the tangent plane to the sphere by a CD-grid-type finite element, JAMES (2022), e2022MS003010.
- [7] Y. Shih et al., Robust and efficient primal-dual Newton-Krylov solvers for viscous-plastic sea-ice models, J. Comput. Phys., 474 (2023), 111802.
- [8] C. Mehlmann, Analysis of the Crouzeix-Raviart surface finite element method for vectorvalued Laplacians, arXiv:2312.16541.

#### Analysis of a viscoplastic Burgers equation

Marita Thomas

(joint work with Xin Liu, Edriss Titi)

This contribution reports on our ongoing study of a viscous Burgers equation, where the viscosity is governed by a positively 1-homogeneous, convex potential and thus leads to a stress in terms of its set-valued subdifferential. This problem is motivated by the so-called Hibler's sea ice model, see [1] and e.g. [2] or [3] for first analytical results on different regularized versions thereof. Hibler's sea ice model treats sea ice as a non-Newtonian fluid, where the stress tensor includes

such a multi-valued term in order to account for the plastic response of the ice. Our simplified model is formulated in one space dimension, on the whole real line; more precisely, we are concerned with in the following Cauchy problem:

(1a) 
$$\partial_t u + \partial_x \left( u^2 / 2 - \sigma \right) = 0$$
 in  $(0, \infty) \times \mathbb{R}$ , where

(1b) 
$$\sigma(t,x) \in \partial \psi(\partial_x u(t,x)) \quad \text{with } \psi(a) = |a| \text{ for } a \in \mathbb{R},$$

complemented by the following far-field boundary condition

(1c) 
$$\lim_{|x| \to \infty} u(t, x) = 0 \quad \text{ for all } t \in [0, \infty),$$

and by the following initial condition

(1d) 
$$u(0,x) = u_{\rm in}(x)$$
 for all  $x \in \mathbb{R}$ .

Above in (1b), the set-valued subdifferential of the convex, positively 1-homogeneous potential  $\psi$  takes the form

$$\partial \psi(a) \left\{ \begin{array}{ll} = \{-1\} & \text{if } a < 0 \,, \\ \in [-1, 1] & \text{if } a = 0 \,, \\ = \{+1\} & \text{if } a > 0 \,. \end{array} \right.$$

For this simplified one-dimensional model (1) given by the viscoplastic Burgers equation we introduce a suitable notion of solution in the framework of BV-solutions, study their existence, and further investigate their properties in [4].

The viscous Burgers equation  $\partial_t u_\varepsilon + \partial_x \left(u_\varepsilon^2/2 - \varepsilon \partial_x u\right) = 0$  and the inviscid Burgers equation  $\partial_t u_\varepsilon + \partial_x u_\varepsilon^2/2 = 0$  as its vanishing viscosity limit are well-understood in classical literature on first-order conservation laws using the notion of BV-solutions. Instead, problem (1) in absence of the convection term  $\partial_x u_\varepsilon^2/2$  forms a gradient flow. In [5] the authors succeeded to study it as an  $L^2$ -gradient flow of the total variation functional for functions of bounded variation on bounded domains. The main challenge in the mathematical analysis of the viscoplastic Burgers model (1) lies in the combined presence of the convection term and the stress  $\sigma$  stemming from the non-smooth potential  $\psi$ , which thus couples the Hamiltonian part and the non-smooth, dissipative part. It is well-known that shocks form in the inviscid Burgers equation, which are still suppressed in the viscous version. In [6] the authors studied a variant of the viscous Burgers equation, where the quadratic viscous potential  $\psi_2(a) := \frac{1}{2}|a|^2$  was replaced by

(2) 
$$\psi_{\varepsilon}(a) := \sqrt{|a|^2 + \varepsilon^2}$$

with  $\varepsilon = 1$ , and observed that large gradients lead to jumps. In other words, the parabolicity of this problem is too weak to prevent shocks for near-shock data. We observe a similar behavior for our less regular potential  $\psi$ . Therefore [4] in particular investigates the interplay of shock waves with the non-smoothness.

In order to obtain the existence of BV-solutions for (1) we approximate (1) by a sequence of regularized problems featuring a small parameter  $\varepsilon > 0$ ; in particular,

the regularized version of (1a), (1b) reads

(3a) 
$$\partial_t u_{\varepsilon} + \partial_x \left( u_{\varepsilon}^2 / 2 - \sigma_{\varepsilon} - \varepsilon \partial_x u_{\varepsilon} \right) = 0 \quad \text{in } (0, \infty) \times \mathbb{R}, \quad \text{where}$$

(3b) 
$$\sigma_{\varepsilon}(t,x) = D\psi_{\varepsilon}(\partial_x u_{\varepsilon}(t,x)) \text{ for } \psi_{\varepsilon} \text{ from (2)},$$

again complemented by far-field boundary and initial conditions. In this way, the multivalued subdifferential is replaced in (3) by the Fréchet derivative of the smooth potential  $\psi_{\varepsilon}$ . Additionally, the regularized model (3) features a viscous regularization stemming from the quadratic viscous potential  $\psi_{\varepsilon}^{\varepsilon}(a) = \frac{\varepsilon}{2}|a|^2$ . For  $\varepsilon > 0$  we obtain local-in-time  $H^2$ -solutions and a-priori bounds uniform in  $\varepsilon$  from the energy-dissipation balance of the regularized problems. Based on this, we establish in [4] a suitable notion of BV-solution for problem (1) that arises from a weak formulation of (3) in the limit  $\varepsilon \to 0$ . In particular, the term  $\sigma$  arises as the limit of the sequence  $(D\psi_{\varepsilon}(\partial_x u_{\varepsilon}))_{\varepsilon}$  and it can be related to an element of the subdifferential of the total variation functional defined on a suitable subspace of a Bochner space with values in the space of functions of bounded variation. We derive the Rankine-Hugoniot condition at jumps and a suitable entropy condition for piecewise smooth solutions.

This is joint work in progress with Xin Liu (Texas A&M University) and Edriss Titi (Texas A&M University and University Cambridge), supported by the DFG within project C09 Dynamics of Rock Dehydration on Multiple Scales of CRC 1114 Scaling Cascades in Complex Systems, project number 235221301.

### References

- W.D. Hibler, A dynamic thermodynamic sea ice model, J. Phys. Oceanogr. 9(4) (1979), 815–846.
- [2] X. Liu, M. Thomas, and E. Titi, Well-Posedness of Hibler's Dynamical Sea-Ice Model, J. of Nonlinear Science 32 (2022), article number 49.
- [3] F. Brandt, K. Disser, R. Haller-Dintelmann, and M. Hieber, Rigorous Analysis and Dynamics of Hibler's Sea Ice Model, J. Nonlinear Science 32 (2022), article number 50.
- [4] X. Liu, M. Thomas, and E. Titi, On the viscoplastic Burgers equation, in preparation (2025).
- [5] M.H. Giga, Y. Giga, and R. Kobayashi, Very Singular Diffusion Equations, Adv. Stud. Pure Math. (2001), 93-125.
- [6] A. Kurganov and P. Rosenau, Effects of a Saturating Dissipation in Burgers-Type Equations, Communications on Pure and Applied Mathematics 50(8) (1997), 753–771.

### Eye formation in tropical cyclones

Emmanuel Dormy

(joint work with Peter A. Davidson, Kerry A. Emanuel, Ludivine Oruba and Andrew M. Soward)

The eye is probably the most striking property of a hurricane, yet its origin is poorly understood. I have reported in this presentation the investigation of a simplified mathematical model of the atmosphere: dry rotating Rayleigh-Bénard

convection under the Boussinesq approximation. More precisely, the flow is governed by

(1) 
$$\frac{\mathrm{D}\boldsymbol{u}}{\mathrm{D}t} = -\frac{1}{\rho_0}\nabla p - 2\boldsymbol{\Omega} \times \boldsymbol{u} + v\nabla^2\boldsymbol{u} - \alpha\theta\boldsymbol{g}, \quad \text{with } \nabla \cdot \boldsymbol{u} = 0,$$

which is complemented by an advection diffusion equation for the temperature perturbation  $\theta$ . If we restrict our attention to an axisymmeric flow, which is a sensible simplified model for a tropical cyclone (TC), the azimuthal component of (1) then yields an evolution equation for the angular momentum  $\Gamma = ru_{\phi}$ ,

(2) 
$$\frac{\mathrm{D}\Gamma}{\mathrm{D}t} = -2r\Omega u_r + v\nabla_{\star}^2(\Gamma),$$

where  $\nabla_{\star}^2$  is the 'Stokes operator', defined as  $\nabla_{\star}^2 = r \frac{\partial}{\partial r} \left( \frac{1}{r} \frac{\partial}{\partial r} \right) + \frac{\partial^2}{\partial z^2}$ . While the curl of the poloidal components yields an evolution equation for the azimuthal vorticity,  $\boldsymbol{\omega}_{\phi} = \boldsymbol{\nabla} \times \boldsymbol{u}_{p}$ ,

(3) 
$$\frac{\mathrm{D}}{\mathrm{D}t} \left( \frac{\omega_{\phi}}{r} \right) = \frac{\partial}{\partial z} \left( \frac{\Gamma^2}{r^4} \right) + \frac{2\Omega}{r} \frac{\partial u_{\phi}}{\partial z} - \frac{\alpha g}{r} \frac{\partial \theta}{\partial r} + \frac{\nu}{r^2} \nabla_{\star}^2 \left( r \omega_{\phi} \right) .$$

An isolated cyclone in a cylindrical domain is being investigated numerically. The domain is bounded introducing an artificial outer wall, which is not present in the geophysical setup. It is shown that the use of stress-free boundary conditions on this wall results in the formation of a singularity [4], no-slip boundary conditions therefore must be considered. Numerical simulations are performed on which eye formation can be investigated [2, 3]. Different boundary conditions, of increasing geophysical relevance, as well as a simplified model for radiative cooling are also investigated [1].

Equation (3) is enlightening. The eyewall is characterised by a strong negative azimuthal vorticity (associated with the rapid upwelling in the eyewall and the slow subsidence within the eye). On the right-hand-side of (3) four terms are present, from left to right, the so-called vortex tilting term, the Coriolis term, the buoyancy term and the viscous term. Numerical simulations reveal that locally, near the eye, both the Coriolis term and the buoyancy term are secondary. The leading order balance involves the non-linear advection (on the left-hand side), the vortex tilting term and the viscous stress. In the limit of low viscosity (relevant to TCs away from boundary layers) it is easy to show that the vortex tilting term cannot, in this model, cause any net negative azimuthal vorticity in the eyewall. Indeed, (3) yields

(4) 
$$\nabla \cdot \left(\frac{\omega_{\phi}}{r}\mathbf{u}\right) = \frac{\partial}{\partial z} \left(\frac{\Gamma^2}{r^4}\right),$$

considering a flux tube  $\mathcal{F}$ , bounded by two streamlines and by a fixed radius  $r_e$  in the (r, z) plane, and integrating (4) over this tube, by Fubini, the right-hand side involves an integral in z at fixed r of  $(\partial/\partial z) (\Gamma^2/r^4)$ . Because  $\Gamma$  is constant on each bounding streamline, this integral vanishes for each value of r and so does the right-hand side of (4). This shows that the vortex tilting term (involving axial gradients in  $\Gamma$ ) has no net contribution to the azimuthal vorticity

in the eyewall. An eye formation mechanism relying on vorticity stripping from the bottom boundary layer is thus identified. It does differ from earlier models which either involve diabatic heating or rely on the vortex tilting term.

As an illustration, a standard discussion of the eye formation could consider the cyclostrophic approximation in the radial direction together with the hydrostatic balance in the vertical direction. This would correspond in our model to balancing the first and the third term on the RHS of (3). We have however observed numerically that the third term (buoyancy) was unimportant in the local dynamics, and we have further observed that the (non-hydrostatic) vertical advection was very significant near the eyewall.

A first attempt to derive an asymptotic solution (based on the small aspect ratio of the domain) has been provided in [5]. While the asymptotic solution can capture important features of the flow near onset, because the solution involves separation of variables, it cannot allow the description of the eye. This mechanism is thus currently lacking a formal mathematical description.

It is also important to stress that this mechanism has only been highlighted in a dry model of TC. In our model, motions are solely driven by heat and the atmosphere therefore needs to be unstably stratified. Models involving moist convection are currently under development to test whether this mechanism could still drive subsidence in the presence of diabatic heating, and if not, how the force balance is modified by the release of latent heat via condensation.

#### References

- E. Dormy, L. Oruba and K.A. Emanuel, Eye Formation and energetics in a dry model of hurricane-like vortices, Journal of the Atmospheric Sciences, 81 (2024), 1565-1578.
- [2] L. Oruba, P.A. Davidson, E. Dormy, Eye formation in rotating convection J. Fluid Mech., 812 (2017), 890–904.
- [3] L. Oruba, P.A. Davidson, E. Dormy, Formation of eyes in large-scale cyclonic vortices, Phys. Rev. Fluids, 3 (2018), 013502.
- [4] L. Oruba, A.M. Soward and E. Dormy, Spin-down in a rapidly rotating cylinder container with mixed rigid and stress-free boundary conditions, J. Fluid Mech., 818 (2017), 205–240.
- [5] A.M. Soward, L. Oruba and E. Dormy, Bénard convection in a slowly rotating penny shaped cylinder subject to constant heat flux boundary conditions, J. Fluid Mech., 951 (2022), A5.

## The three limits of the hydrostatic approximation

Amru Hussein

(joint work with Ken Furukawa, Yoshikazu Giga, Matthias Hieber, Takahito Kashiwabara, Marc Wrona)

The primitive equations are derived from the 3D-Navier-Stokes equations by the hydrostatic approximation. Formally, assuming a vertically  $\varepsilon$ -thin domain

$$\Omega_{\varepsilon} := (-1, 1) \times (-1, 1) \times (-\varepsilon, \varepsilon), \text{ where } \varepsilon > 0,$$

and anisotropic viscosities with vertical viscosity  $\nu_z(\varepsilon)$  and horizontal viscosity  $\nu_H = 1$ , one obtains the rescaled Navier-Stokes equations on  $\Omega_1 \times (0,T)$  for T > 0  $(NS_{\varepsilon,\delta})$ 

$$\begin{cases} \partial_t v_{\varepsilon,\delta} + u_{\varepsilon,\delta} \cdot \nabla v_{\varepsilon,\delta} - \Delta_H v_{\varepsilon,\delta} - \frac{\nu_z(\varepsilon)}{\varepsilon^2} \partial_z^2 v_{\varepsilon,\delta} + \nabla_H p_{\varepsilon,\delta} = 0, \\ \varepsilon^2 \left( \partial_t w_{\varepsilon,\delta} + u_{\varepsilon,\delta} \cdot \nabla w_{\varepsilon,\delta} - \Delta_H w_{\varepsilon,\delta} - \frac{\nu_z(\varepsilon)}{\varepsilon^2} \partial_z^2 w_{\varepsilon,\delta} \right) + \partial_z p_{\varepsilon,\delta} = 0, \\ \operatorname{div} u_{\varepsilon,\delta} = 0, \\ u_{\varepsilon,\delta}(0) = (u_0)_{\varepsilon,\delta}. \end{cases}$$

The formal limit equation for  $\varepsilon \to 0$  now depends crucially on the behaviour of the term

$$\delta := \frac{\nu_z(\varepsilon)}{\varepsilon^2}.$$

For  $\varepsilon \to 0$  one hence has three cases: For  $\delta > 0$  constant setting for simplicity  $\delta = 1$ , one has formally the primitive equations with full viscosity as  $\frac{\nu_z(\varepsilon)}{\varepsilon^2} = 1$ . If  $\delta \to 0$ , one obtains the primitive equations with only horizontal viscosity as in  $(\mathrm{NS}_{\varepsilon,\delta})$  also the term  $\frac{\nu_z(\varepsilon)}{\varepsilon^2}\partial_z^2v_\varepsilon \to 0$  for  $\delta \to 0$ . In the case  $\delta \to \infty$  one obtains the 2D-Navier-Stokes equations which can be seen heuristically when considering the energy inequality. The convergence for  $\delta = \delta_\varepsilon = \varepsilon^{\gamma-2}$  and  $\varepsilon \to 0$  for  $\gamma > 2$  has been proven recently by Li, Titi, and Yuan using energy estimates. Here, we consider more generally  $\nu_z = \varepsilon^2 \delta$  and show how maximal regularity methods and quadratic inequalities can be an efficient approach to the same end for  $\varepsilon, \delta \to 0$  in the strong setting. The flexibility of our methods is also illustrated by the convergence for  $\delta \to \infty$  and  $\varepsilon \to 0$  to the 2D-Navier-Stokes equations.

## On the stationary triple-deck equations

Yasunori Maekawa (joint work with Sameer Iver)

The triple-deck equations are a classical boundary layer model which describes the asymptotics of a viscous flow near the separation point, and the Couette flow is an exact stationary solution to the triple-deck equations. In this talk we see some key mathematical structures of two-dimensional stationary triple-deck system in the half space: the kinetic operator which is well known as hypoeliptic, nonlinear transport effect away from the boundary, and the elliptic regularization of the order 4/3 for the unknown variable related to the pressure-displacement relation. These structures lead to the local rigidity theorem of the Couette flow in the sense that there are no other stationary solutions near the Couette flow in a scale invariant space. This result provides a stark contrast to the well-studied stationary Prandtl counterpart, and in particular offers a first result towards the rigidity question raised by R. E. Meyer in 1983.

#### References

 S. Iyer and Y. Maekawa, Local Rigidity of the Couette Flow for the Stationary Triple-Deck Equations. arXiv:2405.10532 [math.AP]

## Mathematical analysis of an inviscid Voigt regularisation of the elastic-viscous-plastic sea-ice model

Daniel W. Boutros

(joint work with Xin Liu, Marita Thomas and Edriss S. Titi)

We consider the elastic-viscous-plastic (EVP) sea-ice model, which was originally introduced in [1] and is one of the most frequently used and standard dynamical sea-ice models. In particular, we introduce an inviscid Voigt-regularisation (i.e. a term  $-\alpha^2 \partial_t \Delta \sigma$ ) of the evolution equation of the stress tensor, which leads us to consider the following (regularised) Voigt-EVP model

(1)  $\partial_t u = \nabla \cdot \sigma + \mathcal{T}$ ,

(2) 
$$\frac{1}{\mathcal{E}} \partial_t \left( \sigma - \alpha^2 \Delta \sigma \right) + \frac{4\mathcal{D}_{\epsilon}}{P} \left( \sigma - \frac{1}{2} \operatorname{Tr} \sigma \mathbb{I}_2 \right) + \frac{\mathcal{D}_{\epsilon}}{2P} \operatorname{Tr} \sigma \mathbb{I}_2 + \frac{\mathcal{D}_{\epsilon}}{2} \mathbb{I}_2 = D(u),$$

(3) 
$$u|_{t=0} = u_0, \quad \sigma|_{t=0} = \sigma_0,$$

where  $u: \mathbb{T}^2 \times [0,T] \to \mathbb{R}^2$  is the velocity field,  $\sigma: \mathbb{T}^2 \times [0,T] \to \mathbb{R}^{2 \times 2}$  is the stress tensor,  $\mathcal{T}: \mathbb{T}^2 \times [0,T] \to \mathbb{R}^2$  includes the wind and ocean stresses, as well as the Coriolis and gravitational forces. Moreover, P>0 is the pressure,  $\alpha>0$  is the (Voigt) regularisation parameter and  $\mathcal{D}_{\epsilon}=\sqrt{|D(u)|^2+\epsilon^2}$  is the (regularised) strain rate, where  $D(u)=\frac{1}{2}[\nabla u+(\nabla u)^{\top}]$  is the symmetric part of the gradient and  $\epsilon\geq0$  is the strain rate cutoff parameter.

First we observe that without the Voigt regularisation, the linearised 1D EVP model (around a solution  $(\overline{u}, \overline{\sigma})$ ) is (locally) elliptic if at a space-time point  $(x_0, t_0)$ 

$$1 - \frac{5}{2P} \frac{\overline{\sigma} \partial_x \overline{u}}{\sqrt{|\partial_x \overline{u}|^2 + \epsilon^2}} - \frac{1}{2} \frac{\partial_x \overline{u}}{\sqrt{|\partial_x \overline{u}|^2 + \epsilon^2}} < 0.$$

This linear instability of the 1D EVP model will be studied in a forthcoming paper and leads us to consider the Voigt-EVP model (1)-(3).

In [2] we prove the global well-posedness of the Voigt-EVP model. In particular, for  $u_0 \in H^2(\mathbb{T}^2)$  and  $\sigma_0 \in H^3(\mathbb{T}^2)$  (and reasonable assumptions on the drag forces) we show that there exists a unique global strong solution  $(u, \sigma) \in C([0,T];H^2(\mathbb{T}^2)) \times C([0,T];H^3(\mathbb{T}^3))$ . In particular, we are also able to prove the global well-posedness of the system for the case of strain rates without cutoff (i.e. when  $\epsilon = 0$ ), which has been a major issue in the computational study and analysis of the related Hibler sea-ice model.

#### References

- E. C. Hunke and J. K. Dukowicz, An elastic-viscous-plastic model for sea ice dynamics, Journal of Physical Oceanography 27 (1997), 1849–1867.
- [2] D. W. Boutros, X. Liu, M. Thomas and E. S. Titi, Global well-posedness of the elastic-viscous-plastic sea-ice model with the inviscid Voigt-regularisation, arXiv:2505.03080 (2025), 1–26.

### Analysis aspect of tropical climate model

Dongjuan Niu

(joint work with Huiru Wu, Robin Ming Chen, Houzhi Tang)

The study of large-scale atmospheric and oceanic flows is essential for understanding tropical climate dynamics, where interactions between barotropic and baroclinic velocity modes and temperature variations play a significant role. To address this, Frierson, Majda, and Pauluis [3] introduced the tropical climate model (TCM), which was derived from the hydrostatic Boussinesq equations via Galerkin truncation up to the first baroclinic mode for understanding key dynamical processes in tropical climates.

In this talk, I will primarily present the mathematical theory of TCM, which includes its well-posedness, large-time behavior, and nonlinear stability around the shear flows. Precisely, I first introduce the global well-posedness and large-time behavior of 2D TCM under smallness assumption of the initial data. To explore the intrinsic relationship between the first baroclinic mode of the velocity and temperature, we further investigate the stability around the steady-state solution and the optimal time decay rates for 3D TCM. The key points here are that we remove the smallness assumption on the lower-frequency part of the initial data and establish both the upper and lower bounds of the time decay rate. Finally, we prove the nonlinear stability around the Couette flow for 2D viscous TCM by virtue of the enhanced dissipation generated by the non-self-adjoint operator  $y\partial_x - \Delta$ . In this proof, we utilize the method of Fourier multiplier operators to achieve additional regularity, which was first introduced by Deng-Wu-Zhang [2] for Boussinesq equations and later developed by Wei-Zhang [6] for Navier-Stokes equations.

- [1] R. Chen, D. Niu, T. Tang, H. Wu, Stability and optimal decay for the 3D tropical climate model with damping, to appear in J. Differ. Equ. (2025).
- [2] W. Deng, J. Wu, P. Zhang, Stability of Couette flow for 2D Boussinesq system with vertical dissipation, J. Funct. Anal. 281 (2021), 109255.
- [3] D. Frierson, A. Majda, O. Pauluis, Large scale dynamics of precipitation fronts in the tropical atmosphere: a novel relaxation limit, Commun. Math. Sci., 2 (2004), 591–626.
- [4] D. Niu, H. Wu, Stability of Couette flow for 2D tropical climate system with zero thermal dissipation, Nonlinearity 38 (2025), no. 1, Paper No. 015017, 13 pp.
- [5] D. Niu, H. Wu, Global strong solutions and large-time behavior of 2D tropical climate model with zero thermal diffusion, Math. Methods Appl. Sci 45 (2022), no. 16, 16, 9341–9370.

[6] D. Wei, Z. Zhang, Nonlinear enhanced dissipation and inviscid damping for the 2D Couette flow, Topology 5 (2023), no. 3, 573–592.

## Variational Closures Of Composite Homogenised Fluid Flows Ruiao Hu

(joint work with Theo Diamantakis, James-Michael Leahy)

Stochasticity arises naturally in the modelling of multiscale systems. Theoretically, it emerges in the singular limits of systems with multiple temporal and spatial scales. In applications such as geophysical fluid dynamics, stochasticity can effectively represent unresolved turbulent fluctuations and their feedback on resolved scales.

In this talk, based on the preprint [1], we apply homogenisation theory to derive a Lagrange-to-Euler map of an ideal fluid flow, modelled by a stochastic flow of diffeomorphisms, as the deterministic homogenised limit of a parameterised flow map that decomposes into rapidly fluctuating and slow components in time. In this limit, the rapidly fluctuating component becomes a prescribed stochastic flow of diffeomorphisms that can introduce stochasticity into the dynamics of the slow component, which are closed through Euler-Poincaré variational principles [3].

By constraining the variations to adhere to the composite structure of the stochastic flow of diffeomorphisms derived from the homogenisation limit, we obtain stochastic partial differential equations for fluid momentum and tracers with transport noise agreeing with those derived in, e.g., [2]. We show that these stochastic equations are equivalent to a system of random coefficient partial differential equations for the mean fluid momentum and tracers via a transform by the stochastic flow of diffeomorphisms. Owing to its variational derivation, this result holds for a large class of geophysical fluid models outlined in [3] and we illustrate it through Euler's equation.

- [1] T. Diamantakis and R. Hu, Variational closures for composite homogenised fluid flows. arXiv preprint (2024), arXiv:2409.10408.
- [2] D. D. Holm, Variational principles for stochastic fluid dynamics. Proceedings of the Royal Society A 471 (2015), 20140963.
- [3] D. D. Holm, J. E. Marsden, and T. S. Ratiu, The Euler-Poincaré Equations and Semidirect Products with Applications to Continuum Theories. Advances in Mathematics, 137 (1998), 1–81, 7.

## Stochastic geometric mechanics and its application to transport noise in continuum dynamics

OLIVER D. STREET

Stochastic modelling approaches have the ability to provide a statistical representation of the influence of unresolved physical processes on those resolved within computational simulations of large-scale fluid systems. The stochastic modelling approach is most applicable to multiscale systems, such as the climate [2], which have both slow and fast dynamics interacting nonlinearly.

When stochastic forcing terms are incorporated into the classical equations of fluid mechanics, care must be taken to ensure that the mathematical structure of the model is not destroyed. Using the geometric structures inherent to inviscid fluid mechanics, it is possible to add transport noise to continuum models in such a way that many conservation laws of the deterministic system are present in the stochastic case [3]. For example, the vorticity form of Euler's equation becomes

(1) 
$$d\omega + \mathcal{L}_u \omega \, dt + \sum \mathcal{L}_{\xi_i} \omega \circ dW_t^i = 0 \,,$$

where  $\xi_i$  are arbitrary fixed vector fields, and  $\{\circ dW_t^i\}_{i\geq 1}$  denotes Stratonovich integration with respect to i.i.d. Brownian motions. The Lie derivative operator  $\mathcal{L}_u\omega$  is  $u\cdot\nabla\omega$  in 2D and includes the line stretching term in 3D. This equation then conserves enstrophy (in 2D), helicity (in 3D), all Casimirs of the Lie-Poisson bracket, has a Kelvin circulation theorem, but does not preserve energy. A variety of geophysical models have since been derived using this approach.

This approach has recently been shown to provide a stochastic generalisation of the key structures present in geometric mechanics [5], including reduction by symmetry and Noether's theorem, and be consistent with stochastic Hamiltonian systems of the type studied in [1, 4]. Thus, it preserves many conserved quantities of physical models which result from symmetries or degeneracy of the Poisson structure. It remains to explore the breadth of the applicability of this work, and understand which problems are most aided by its ability to preserve structure.

- Bismut, J. -M. (1981) Mécanique aléatoire. Lecture Notes in Mathematics 866. Berlin, Springer.
- [2] Hasselmann, K. (1976) Stochastic climate models Part I. Theory. Tellus. 28, 473-485.
- [3] Holm, D. D. (2015) Variational principles for stochastic fluid dynamics. Proceedings of the Royal Society A. 471, 20140963.
- [4] Lázaro-Camí, J. -A. and Ortega, J. -P. (2008) Stochastic hamiltonian dynamical systems. Reports on Mathematical Physics, 61 (1), 65–122.
- [5] Street, O. D. and Takao, S. (2024) Semimartingale driven mechanics and reduction by symmetry for stochastic and dissipative dynamical systems. arXiv [Preprint].

### Traveling water waves

JÖRG WEBER

In this talk, we give a short introduction to the traveling water wave problem in two dimensions, one of the oldest problems in mathematics with a history of more than two centuries. After presenting the original equations in the spirit of Euler, we rewrite them in the stream formulation, which is more amenable to tools from functional analysis. Here, a handful of key challenges are identified: the a priori unknown fluid domain, making the problem a free boundary problem; the choice of a change of variables to map the domain to a fixed domain; the nonlinear and inherently nonlocal nature of the problem; allowing for various streamline patterns and free surface geometries. Finally, we explain the established strategy of applying abstract (local and global) bifurcation theorems to construct solutions rigorously and discuss open questions in the field, such as characterizing the limiting behavior of a bifurcation branch depending on the vorticity function. For further details see, for example, [1, 2, 3, 4].

### References

- [1] A. and W. A. Strauss, Exact steady periodic water waves with vorticity, Communications on Pure and Applied Mathematics 57.4 (2004), 481–527.
- [2] A. Constantin, W. A. Strauss and E. Vărvărucă, Global bifurcation of steady gravity water waves with critical layers, Acta Mathematica 217.2 (2016), 195–262.
- [3] S. V. Haziot, V. M. Hur, W. A. Strauss, J. F. Toland, E. Wahlén, S. Walsh, and M. H. Wheeler, Traveling water waves—the ebb and flow of two centuries, Quarterly of Applied Mathematics 80.2 (2022), 317–401.
- [4] E. Wahlén and J. Weber, Large-amplitude steady gravity water waves with general vorticity and critical layers, Duke Mathematical Journal 173.11 (2024), 2197–2258.

## On the nonlinear dynamics of Saturn's hexagon

ADRIAN CONSTANTIN (joint work with R. S. Johnson)

The amazing hexagonal structure that surrounds the North Pole of Saturn in a zonal polar band has fascinated scientists since it was first glimpsed in the 1980s. Although several phenomenological models have been able to reproduce such flow patterns, a self-consistent model for how large-scale and high-speed polygonal jets might form in the upper troposphere of is lacking.

Observations show that an assortment of smaller vortices that are caught up in the hexagon's jet-stream rotate clockwise. A strong eastward jet is located within the warm belt between 72°N and 78°N, and the zonal velocity of this sheared jet increases from about 80  $\rm m\,s^{-1}$  at 72°N to nearly 120  $\rm m\,s^{-1}$  at 78°N (see [6]). The poleward directional shear induces vorticity tubes within the belt, veering particles between the boundaries in a clockwise motion. On the other hand, due to the high latitudes, the jet trajectories along the boundaries of the belt are more accurately described as being counterclockwise circular, instead of the straightline-flow model adequate for equatorial regions. This makes hypotrochoids – paths

mapped out by the movement composed of the rotation of two circular motions in opposite directions – dynamically relevant. Note that a purely circular motion captures the salient features of Jupiter's Great Red Spot, while the composition of a straight-line motion and a circular motion describes the filamentary zonal flow that is observed on the southern boundary of the Great Red Spot (see [1]).

We now describe the approach pursued in [2]. It starts with the general equations of motion for compressible, inviscid flow, written in local rectangular coordinates and with the f-plane approximation invoked. We non-dimensionalise and apply a systematic thin-shell asymptotic procedure to derive a consistent set of nonlinear governing equations for the dynamics of flows confined to a thin layer in a narrow, zonal, cloud band. Then we show that the governing equations admit solutions with particles moving on paths shaped like regular polygons with rounded corners, which arise as trajectories of the movement of two circular motions in opposite directions. The available data links the specific number of corners to the internal heat forcing and to the location of the pattern. The obtained solution captures the following observed features (for data see [2, 4, 6]):

- (1) size of the hexagon;
- (2) speeds within the hexagonal jet stream (maximal/minimal zonal speeds of about  $118/82 \text{ m s}^{-1}$  and meridional speeds of about  $18 \text{ m s}^{-1}$ );
- (3) the hexagon is a heat sink (heat flows towards the hexagon);
- (4) the hexagonal band's excursions in latitude are approximately  $\pm 1^{\circ}$ ;
- (5) there is a poleward temperature increase within the hexagonal jet<sup>1</sup> of about 5°K.

On the basis of the results that we have obtained, it is reasonable to conclude that the hexagon is sensitive to, and is controlled by, the internal heat sources. If the heat forcing changes only slightly over a period of Saturnian years – and we have evidence so far for only a little over one Saturnian year – then we can expect that the dynamical structures that we observe at the surface of the atmosphere will remain essentially unaltered. And there is more. Our approach, based on the construction of particle paths, shows that we can not only describe the spectacular hexagonal pattern, but also other structures that are typical of zonal flows on Saturn. Hypotrochoidal paths arise naturally in the sheared zonal flows confined to narrow circumpolar bands that are typical for Saturn, if there is a suitable heat forcing. However, only rounded polygonal patterns (like the hexagon) are easy to track, while other paths present a large number of self-intersections. This also means that under a period change of the internal heat forcing, Saturn's hexagon will most likely become a transient phenomenon: even a small deviation will, with the passage of time, lead to an intensification of the self-intersections, eventually causing the pattern to depart from its current polygonal shape.

Finally, let us note that only an internal heat forcing that persists for a long time can sustain hypotrochoidal paths. This is relevant for the absence of a polygonal pattern in Saturn's southern polar troposphere, despite the presence of a strongly sheared circumpolar jet flowing eastward in the zonal band between 66°S and 70°S,

<sup>&</sup>lt;sup>1</sup>The North Pole is a hot spot in Saturn's upper troposphere.

with a poleward speed increasing from about  $30 \,\mathrm{m\,s^{-1}}$  to a maximal speed of  $100 \,\mathrm{m\,s^{-1}}$  at  $70^{\circ}\mathrm{S}$ . The crucial difference to Saturn's northern polar troposphere is the absence of a persistent internal heat forcing associated with this southern jet.

#### References

- [1] A. Constantin and R. S. Johnson, Nonlinear atmospheric flow patterns confined to zonal cloud bands, J. Atmos. Sci. 82 (2025), 3–15.
- [2] A. Constantin and R. S. Johnson, Nonlinear atmospheric flow patterns confined to zonal cloud bands: Saturn's hexagon, J. Atmos. Sci. (to appear).
- [3] A. P. Ingersoll, "Planetary climates", Princeton University Press, 2013.
- [4] A. P. Ingersoll, Cassini exploration of the planet Saturn: a comprehensive review, Space Sci. Rev. 216 (2020), Art. 122.
- [5] K. R. Meyer, G. R. Hall and D. Offin, "Introduction to Hamiltonian dynamical systems and the N-body problem", Springer, 2009.
- [6] A. Sánchez-Lavega, "An introduction to planetary atmospheres", CRC Press, 2011.
- [7] G. K. Vallis, "Atmospheric and oceanic fluid dynamics", Cambridge University Press, 2017.

## Critical Drift-Diffusion equations: Intermittent behavior

Felix Otto

(joint work with Sefika Kuzgun, Peter Morfe, Christian Wagner)

We are interested in the drift-diffusion equation

(1)  $\partial_t u - b \cdot \nabla u - \Delta u = 0$  in the whole *n*-dimensional space with a time-independent and divergence-free drift *b*, i.e.  $\partial_t b = 0$  and

$$(2) \nabla \cdot b = 0.$$

More precisely, we are interested in the Lagrangian coordinates, that is, the initial data u(t=0,x)=x, and the drift b sampled from a stationary and isotropic Gaussian ensemble. The theme of the work is that Gaussian b induces an intermittent (and thus strongly non-Gaussian) behavior on the level of u. We are able to establish this in the scaling-critical setting

(3) 
$$b(\mu \cdot) = \frac{1}{\mu}b \text{ in law for all } \mu > 0,$$

in which convection and diffusion balance at every scale.

It is well-known that this setting is too rough: By the scale-invariance in law (3), the regularity of b is no better than  $C^{-1}$ , so that in view of (1), u is at best<sup>1</sup> in  $C^{1}$  which is insufficient to define the product  $b \cdot \nabla u = \nabla \cdot ub$ . To remedy this, we consider a small-scale cut-off, w.l.o.g. at scale 1 and implemented on the level of the Fourier transform:

(4) 
$$\mathcal{F}b(k) = 0$$
 for every wave number  $|k| \ge 1$ .

<sup>&</sup>lt;sup>1</sup>In fact our result (5) shows that u is worse than Lipschitz continuous by the quartic root of a logarithm.

This fixes b up to a single constant which we describe in terms of  $\mathbb{E}|b|^2 = \epsilon^2 n$ , where  $\epsilon \ll 1$  can be interpreted as the Péclet number.

We discover the intermittency on the level of the particle pair distance d

$$d^{2}(T,x) := \frac{1}{T} \int_{0}^{T} dt \frac{|u(t,x) - u(t,0)|^{2}}{|x|^{2}},$$

where w.l.o.g. we put one particle at the origin. We monitor  $d^2$  in terms of the effective single particle diffusivity which is given by

$$\lambda(T) := \sqrt{1 + \frac{\varepsilon^2}{2} \ln(1+T)},$$

as was established with increasing precision in [5, 2, 3, 1].

**Theorem 1** (Kuzgun, Morfe, O., Wagner; see [4] for n = 2). For  $\epsilon^2 \lambda(|x|^2) \ll 1$ ,

(5) 
$$\mathbb{E} d^2(T, x) \approx \max \left\{ \frac{\lambda(T)}{\lambda(|x|^2)}, 1 \right\}$$

while for p > 1,

(6) 
$$\mathbb{E} d^{2p}(T,x) \gtrsim \left(\max\left\{\frac{\lambda(T)}{\lambda(|x|^2)},1\right\}\right)^{1+\frac{2}{n+2}(p-1)}.$$

In view of the positive number  $\frac{2}{n+2}$  in the exponent, the pth moments of the squared particle pair distance feature anomalous behavior in p, which amounts to intermittency.

We now give the main idea behind the proof of Theorem 1. If we momentarily neglect the diffusion in (1) by replacing it with

$$\partial_t u + b \cdot \nabla u = 0.$$

then the Jacobian matrix  $F_t := \nabla^{\dagger} u(t,0)$  satisfies

(7) 
$$\frac{dF}{dt} = F_t \nabla b(u(t,0)) \quad \text{and} \quad F_{t=0} = id.$$

Since by (2),  $\nabla b \in \mathfrak{sl}(n) := \{ \operatorname{tr} B = 0 \}$  one has  $F \in \mathbf{SL}(n) := \{ \det F = 1 \}$ .

In fact there is a unique Brownian motion  $\{B_{\tau}\}_{{\tau}\geq 0}$  on the Lie algebra  $\mathfrak{sl}(n)$  and a corresponding diffusion  $\{F_{\tau}\}_{{\tau}\geq 0}$  on the Lie group  $\mathbf{SL}(n)$  such that

- (a) Itô=Stratonovich:  $dF = F_{\tau} \circ dB = F_{\tau} dB$ ,
- (b) Isotropy:  $OF_{\tau} = F_{\tau}O$  in law for all  $O \in O(n)$ ,
- (c) Normalization:  $d\mathbb{E}|F|^2 = 1\mathbb{E}|F_{\tau}|^2 d\tau$ .

In view of (a), F can be considered a tensorial version of the stochastic exponential and as such displays intermittency:

$$\mathbb{E}|F_{\tau}|^{2p} \sim_{n,p} e^{p(1+\frac{2}{n+2}(p-1))\tau}$$
.

Note that the exponent in (6) arises from the linearization of the above exponent at p = 1.

The main ingredient for Theorem 1 is that after a time change  $t \leftrightarrow \tau$  given by

$$\tau(t) = \ln \lambda(t)$$

one has, even in the presence of diffusion,

'quenched noise'  $\nabla b(u(t,0))dt \approx$  'thermal noise'  $dB_{\tau}$ .

**Theorem 2** ([4]). There exists a coupling  $b \leftrightarrow B$  such that for all (x,T) we have

$$\frac{1}{T} \int_0^T dt \mathbb{E} \left| \nabla^{\dagger} u(t,0) - F_{\tau(T)} \right|^2 \lesssim \epsilon^2 \mathbb{E} |F_{\tau(T)}|^2.$$

More precisely,

$$\mathbb{E}\frac{1}{T} \int_0^T dt \frac{1}{|x|^2} |u(x,t) - u(0,t) - F_{\tau(|x|^2),\tau(T)}^{\dagger} x|^2 \lesssim \epsilon^2 \mathbb{E}|F_{0,\tau(T)}|^2$$

where  $F_{\tau^*,\tau}$  is as in (a) started at time  $\tau^*$ .

The proof is based on the method of scale-by-scale homogenization introduced in [3].

Our result shows that the intermittency of the drift-diffusion equation depends less on topology (stream lines of the diverge-free b are closed iff n = 2) and more on geometry ( $\mathbf{SL}(n)$  has less curvature as n increases).

#### References

- [1] S. Armstrong, A. Bou-Rabee, and T. Kuusi, Superdiffusive central limit theorem for a Brownian particle in a critically-correlated incompressible random drift, arXiv preprint arXiv:2404.01115, 2024.
- [2] G. Cannizzaro, L. Haunschmid-Sibitz, and F. Toninelli, log t-superdiffusivity for a Brownian particle in the curl of the 2D GFF, The Annals of Probability, vol. 50, no. 6, pp. 2475–2498, 2022.
- [3] G. Chatzigeorgiou, P. Morfe, F. Otto, and L. Wang, The Gaussian free-field as a stream function: asymptotics of effective diffusivity in infra-red cut-off, to appear in Annals of Probability, 2025.
- [4] P. Morfe, F. Otto, and C. Wagner, A critical drift-diffusion equation: connections to the diffusion on SL(2), arXiv preprint arXiv:2410.15983, 2024.
- [5] B. Tóth and B. Valkó, Superdiffusive bounds on self-repellent Brownian polymers and diffusion in the curl of the Gaussian free field in d = 2, Journal of Statistical Physics, vol. 147, pp. 113–131, 2012.

# What are good solution concepts for the PDEs of fluid mechanics? Simon Markfelder

(joint work with Valentin Pellhammer, Christian Klingenberg, Emil Wiedemann)

The quest for a good solution concept for the PDEs arising in mathematical fluid mechanics is an outstanding open problem. In this talk we consider both the incompressible

(1) 
$$\operatorname{div} v = 0, \\ \partial_t v + v \cdot \nabla v + \nabla p = 0,$$

and the isentropic compressible Euler equations

(2) 
$$\partial_t \varrho + \operatorname{div}(\varrho u) = 0, \\ \partial_t (\varrho u) + \operatorname{div}(\varrho u \otimes u) + \nabla(\varrho^{\gamma}) = 0.$$

It is well known that the study of weak solutions is unavoidable because strong solutions can blow up in finite time (in the compressible case (2) shocks may evolve; in the incompressible case (1) an example for finite time blow-up was given in [5]). Moreover, we rule out weak solutions which do not comply with the energy inequality, and call the remaining weak solutions admissible. Interestingly, with the help of convex integration one has been able to prove non-uniqueness of admissible weak solutions [4, 1]. This non-uniqueness seems to be related to turbulent behaviour of the flow.

The main purpose of this talk is to address the question of how to deal with the fact that admissible weak solutions are not unique. We discuss two kinds of approaches to overcome the lack of uniqueness.

Firstly, one tries to preserve the concept of weak solutions by imposing a selection criterion in order to identify the "right" admissible weak solution. To explain this we look at the compressible case (2). The strategy is to consider 2-D Riemann data (i.e. 1-D Riemann data which are trivially extended to the second dimension) as a test case, and check whether a certain criterion at hand selects the solution which one expects to be the "right" one. More precisely, such a 2-D Riemann problem may be solved by classical means, which yields a solution consisting of shocks, contact discontinuities, and rarefaction waves. One usually expects that this solution (which is also called the 1-D solution) is the "right" one. However, as shown in [1], there exist infinitely many other admissible weak solutions to the same initial data.

In this talk we consider selection criteria regarding maximal energy dissipation (as suggested in [3]), and criteria concerning the action (as suggested in [6, 7]). We explain why these criteria fail to select the 1-D solution as shown in [2] (for the global maximal dissipation criterion), [9] (for the local maximal dissipation criterion) and [10] (for the least action criterion). Consequently, one either has to reconsider one's intuition that the 1-D solution is the "right" solution, or these criteria must be discarded.

The second direction of how to overcome the problem of non-uniqueness of weak solutions is just to accept it as a matter of fact, and develop generalized solution concepts which capture the non-uniqueness of weak solutions. In this talk we explain the notion of maximally turbulent solutions to the incompressible Euler equations (1), which was introduced recently in [8]. We sketch how existence and uniqueness (which has to be understood in a certain sense) of such solutions is proven. Moreover, we demonstrate by considering an example that this notion of solution represents the most spread out collection of weak solutions. Consequently this solution concept endorses the non-uniqueness at the level of weak solutions but still yields a unique object.

## References

- [1] E. Chiodaroli, C. De Lellis and O. Kreml, Global ill-posedness of the isentropic system of gas dynamics, Comm. Pure Appl. Math. 68(7) (2015), 1157–1190.
- [2] E. Chiodaroli and O. Kreml, On the energy dissipation rate of solutions to the compressible isentropic Euler system, Arch. Ration. Mech. Anal. 214(3) (2014), 1019–1049.
- [3] C. Dafermos, The entropy rate admissibility criterion for solutions of hyperbolic conservation laws, J. Differential Equations 14 (1973), 202–212.
- [4] C. De Lellis and L. Székelyhidi Jr., On admissibility criteria for weak solutions of the Euler equations, Arch. Ration. Mech. Anal. 195(1) (2010), 225–260.
- [5] T. Elgindi, Finite-time singularity formation for C<sup>1,α</sup> solutions to the incompressible Euler equations on R<sup>3</sup>, Ann. of Math. (2) 194(3) (2021), 647–727.
- [6] H. Gimperlein, M. Grinfeld, R. J. Knops and M. Slemrod, The least action admissibility principle, Arch. Ration. Mech. Anal. 249(2) (2025), Paper No. 22.
- [7] H. Gimperlein, M. Grinfeld, R. J. Knops and M. Slemrod, On action rate admissibility criteria, arXiv preprint 2503.03491 (2025).
- [8] C. Klingenberg and S. Markfelder and E. Wiedemann, Maximal turbulence as a selection criterion for measure-valued solutions, arXiv preprint 2503.20343 (2025).
- [9] S. Markfelder, A new convex integration approach for the compressible Euler equations and failure of the local maximal dissipation criterion, Nonlinearity 37(11) (2024), 1–60.
- [10] S. Markfelder and V. Pellhammer, Failure of the least action admissibility principle in the context of the compressible Euler equations, arXiv preprint 2502.09292 (2025).

## Inertial Manifolds for Regularized Navier-Stokes Equations

Yanqiu Guo

(joint work with Mohammad Abu Hamed, Ciprian G. Gal, Michael Ilyin, Edriss S. Titi)

One of the central problems in the study of dissipative systems governed by PDEs is whether their long-term dynamics are effectively finite-dimensional and can be captured by a system of ODEs. To address this, Foias, Sell, and Temam introduced the concept of *inertial manifolds*–finite-dimensional, Lipschitz-continuous, invariant manifolds that attract all trajectories of the associated dynamical system exponentially fast. The existence of an inertial manifold for an infinite-dimensional evolution equation provides the best analytical reduction of such a system to a finite-dimensional one. However, it remains an open question whether the Navier–Stokes equations (NSE) admit an inertial manifold.

In this talk, I discuss the existence of inertial manifolds for certain regularized versions of the Navier–Stokes equations.

In the work [1], in collaboration with Abu-Hamed and Titi, we established the existence of inertial manifolds for two subgrid-scale  $\alpha$ -models of turbulence: the simplified Bardina model and the modified Leray- $\alpha$  model, on the two-dimensional periodic domain  $\mathbb{T}^2$ . These models were derived by weakening the convection term in the NSE. We verified a spectral gap condition and employed a number-theoretic result by Richards concerning large gaps between sums of two squares. It remains of interest to investigate the existence of inertial manifolds for other  $\alpha$ -models of turbulence.

Alternatively, one can regularize the NSE by strengthening its diffusion term. In the work [2], in collaboration with Gal, we proved the existence of inertial manifolds for the *hyperviscous Navier–Stokes equations*:

(1) 
$$\partial_t u + (-\Delta)^{\beta} u + (u \cdot \nabla) u + \nabla p = f$$
, with  $\nabla \cdot u = 0$ ,

on  $\mathbb{T}^2$  or  $\mathbb{T}^3$ , provided  $\beta \geq \frac{3}{2}$ . In particular, when  $\beta = \frac{3}{2}$  on  $\mathbb{T}^3$ , the spectral gap condition fails, and we applied the *spatial averaging method* developed by Mallet-Paret and Sell.

To further reduce the value of  $\beta$ , which represents the strength of hyperviscosity in (1), we studied the sparse distribution of integer lattice points in annular regions in  $\mathbb{R}^2$  and  $\mathbb{R}^3$ —a topic of independent interest in number theory. In collaboration with Ilyin [3], we established an optimal result concerning the asymptotic thickness of annuli within which lattice points are sparsely distributed. Building on this property, we proved the existence of an inertial manifold for the hyperviscous NSE (1) on  $\mathbb{T}^2$  when  $\beta > \frac{17}{12}$  [4].

#### References

- M. Abu Hamed, Y. Guo, and E. S. Titi, Inertial manifolds for certain sub-grid scale alphamodels of turbulence, SIAM J. Appl. Dyn. Syst. 14 (2015), 1308–1325.
- [2] C. G. Gal and Y. Guo, Inertial manifolds for the hyperviscous Navier-Stokes equations, J. Differential Equations 265 (2018), 4335–4374.
- [3] Y. Guo and M. Ilyin, Sparse distribution of lattice points in annular regions, J. Number Theory 264 (2024), 277–294.
- [4] Y. Guo, Inertial manifolds for the two-dimensional hyperviscous Navier-Stokes equations, arXiv:2401.14642 [math.AP] (2024).

## The Dynamics of Stochastically-Forced Beta-Plane Zonal Jets

Laura Cope

(joint work with Peter H. Haynes)

Zonal jets are strong and persistent east-west flows that arise spontaneously in planetary atmospheres and oceans. They are ubiquitous, with key examples including mid-latitude jets in the troposphere, multiple jets in the Antarctic Circumpolar Current and flows on gaseous giant planets such as Jupiter and Saturn. Turbulent flows on a beta-plane lead to the spontaneous formation and equilibration of persistent zonal jets [3]. However, the equilibrated jets are not steady and

the nature of the time variability in the equilibrated phase is of interest both because of its relevance to the behaviour of naturally occurring jet systems and for the insights it provides into the dynamical mechanisms operating in these systems.

#### 1. Mathematical Model

This work discusses aspects of zonal jet variability using insights from a framework of barotropic beta-plane models in which stochastic forcing  $\xi$  generates an idealisation of turbulence. The overarching nonlinear (NL) model can be described using the stochastically-forced, linearly-damped, beta-plane vorticity equation:

(1) 
$$\frac{\partial \zeta}{\partial t} + J(\psi, \zeta) + \beta \frac{\partial \psi}{\partial x} = \xi - \mu \zeta + \nu_n \nabla^{2n} \zeta,$$

where  $\zeta$  is the relative vorticity,  $\psi$  is the streamfunction,  $\xi$  injects energy at rate  $\varepsilon$ ,  $\mu$  is the rate of energy dissipation and  $\beta$  is the potential vorticity gradient. Note that J is the Jacobian determinant, defined by  $J(A, B) = A_x B_y - A_y B_x$ .

This system admits a variety of solutions as the parameters  $(\varepsilon, \mu, \beta)$  are varied. Notably, jets are observed to randomly wander, merge and nucleate, and also to systematically migrate north or south (see figure 1). Whilst jet migration has previously been observed in more complex systems in which there is spherical geometry [1], it has never been observed in a model where there is no obvious latitudinal symmetry breaking mechanism. Numerical data highlights a striking relationship between the jet migration speed,  $\mathcal{V}$ , the dissipation rate,  $\mu$ , and the Rhines scale,  $L_{Rh} \sim \varepsilon^{1/4}/(\beta^{1/2}\mu^{1/4})$  (associated with the jet spacings):

$$(2) \mathcal{V} \sim \mu L_{Rh}.$$

#### 2. Quasilinear and generalized quasilinear models

In order to elucidate aspects of variability, this study uses a hierarchy of model reductions by systematically eliminating nonlinear interactions in the NL model. For simplicity with notation, the NL vorticity equation can be written as

(3) 
$$\partial \zeta / \partial t = \mathcal{L}[\zeta] + \mathcal{N}[\zeta, \zeta],$$

where  $\mathcal{L}$  represents linear operators and  $\mathcal{N}$  includes nonlinear terms of quadratic order. To proceed, a generalisation of a standard Reynolds decomposition is applied to the vorticity field to separate it into two parts: one that is associated

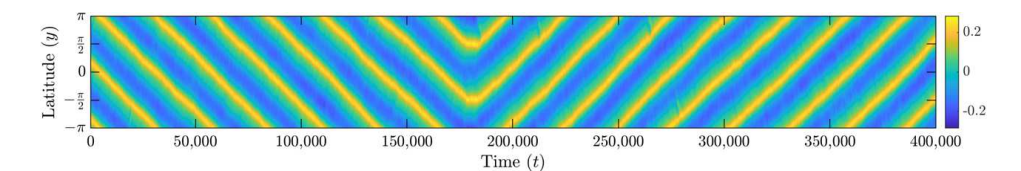


FIGURE 1. A latitude-time plot illustrating the zonal mean zonal flow from the NL model. A pair of jets equilibrate and systematically migrate either north or south, occasionally and spontaneously changing their direction of migration.

with low zonal wavenumber modes,  $\overline{\zeta}^L$ , and one that is associated with high zonal wavenumber modes,  $\overline{\zeta}^H$ , where  $\zeta = \overline{\zeta}^L + \overline{\zeta}^H$ . This decomposition separates the *low modes*, with zonal wavenumbers  $|k_x| \leq \Lambda$ , from the *high modes*, in which  $|k_x| > \Lambda$ :

(4) 
$$\overline{\zeta}^{L}(\mathbf{x},t) = \sum_{|k_{x}| < \Lambda} \sum_{k_{y}} \zeta(\mathbf{k},t) e^{i\mathbf{k} \cdot \mathbf{x}},$$

(5) 
$$\overline{\zeta}^{H}(\mathbf{x},t) = \sum_{|k_x| > \Lambda} \sum_{k_y} \zeta(\mathbf{k},t) e^{i\mathbf{k} \cdot \mathbf{x}},$$

thereby introducing a new parameter,  $\Lambda$ , which is a partition wavenumber representing the largest zonal wavenumber retained in the low modes.

Equations of motion for the low and high modes can be derived, and nonlinear interactions are systematically neglected, as described in [4], such that the system retains the original conservation laws:

(6) 
$$\frac{\partial \overline{\zeta}^{L}}{\partial t} = \mathcal{L}[\overline{\zeta}^{L}] + \overline{\mathcal{N}}^{L}[\overline{\zeta}^{H}, \overline{\zeta}^{H}] + \overline{\mathcal{N}}^{L}[\overline{\zeta}^{L}, \overline{\zeta}^{L}] + \underbrace{\overline{\mathcal{N}}^{L}[\overline{\zeta}^{L}, \overline{\zeta}^{H}]}_{\text{Neglect}},$$

(7) 
$$\frac{\partial \overline{\zeta}^{H}}{\partial t} = \mathcal{L}[\overline{\zeta}^{H}] + \overline{\mathcal{N}}^{H}[\overline{\zeta}^{L}, \overline{\zeta}^{H}] + \underbrace{\overline{\mathcal{N}}^{H}[\overline{\zeta}^{L}, \overline{\zeta}^{L}] + \overline{\mathcal{N}}^{H}[\overline{\zeta}^{H}, \overline{\zeta}^{H}]}_{\text{Neglect}}.$$

This is known as the generalised quasilinear (GQL) approximation. In the limit  $\Lambda \to \infty$ , the high modes disappear,  $\overline{\zeta}^H = 0$ , and we recover the NL model, whilst in the opposite limit,  $\Lambda = 0$  is known as the quasilinear (QL) approximation [5].

Data from a large number of numerical simulations employing the GQL and QL approximations are compared with equivalent NL simulations. Randomly wandering and merging and nucleating behaviours are observed for all  $\Lambda$  values, whilst migrating behaviour only occurs when  $\Lambda \geq 1$ .

## 3. The importance of zonons

These findings highlight the importance of the zonal wavenumber  $k_x=1$  modes, which are a generalization of Rossby waves known as zonons. To highlight their importance more widely, it is possible to construct a simple relationship between the jet strength, sometimes referred to as the zonal mean flow (zmf) index [5], and the dimensionless zonostrophy parameter, defined as  $R_{\beta} \sim \varepsilon^{1/20} \beta^{1/10} / \mu^{1/4}$ :

(8) 
$$\operatorname{zmf} = \frac{R_{\beta}^{10/3}}{6 + R_{\beta}^{10/3}},$$

plotted in figure 2. In simulations where the jet strength is defined to be the zonal mean flow (i.e. zmf), figure 2(a) shows that the jets are weaker than predicted, i.e. the data lie below this curve, and there is a systematic dependency on the type of variability. However, by including the  $k_x = 1$  wavenumbers associated with zonons

in a generalization of this index (gzmf) in figure 2(b), all data closely follow the expected relationship. Further details and references can be found within [2].

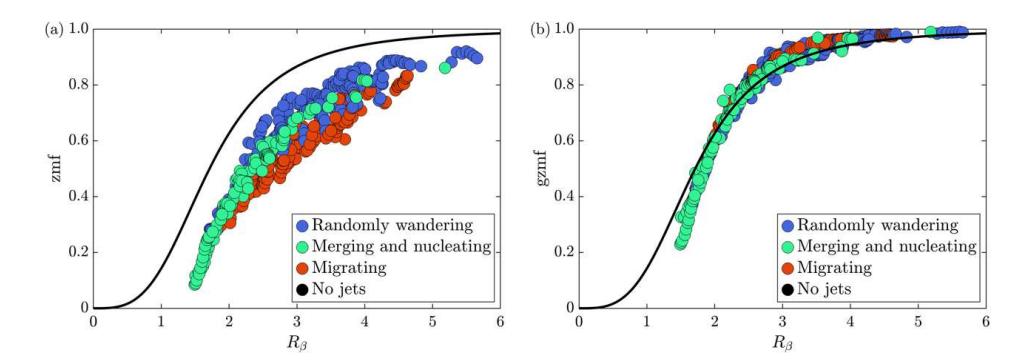


FIGURE 2. The relationship between the zonostrophy parameter,  $R_{\beta}$ , and (a) the zmf index and (b) the gzmf index for 629 NL simulations. Each point represents a single simulation in which the type of variability is denoted by the colour. The black curve plots the theoretical relationship (8).

#### References

- R. Chemke and Y. Kaspi, Poleward migration of eddy-driven jets, Journal of Advances in Modeling Earth Systems 7 (2016), 1457–1471.
- [2] L. Cope, The Dynamics of Geophysical and Astrophysical Turbulence, [Apollo University of Cambridge Repository]. https://doi.org/10.17863/CAM.75705 (2020).
- [3] B. Galperin and P. L. Read (eds), Zonal Jets: Phenomenology, Genesis, and Physics, Cambridge University Press (2019).
- [4] J. B. Marston, G. P. Chini and S. M. Tobias, Generalized quasilinear approximation: Application to Zonal Jets, Physical Review Letters 116 (2016), 214501.
- [5] K. Srinivasan and W. R. Young, Zonostrophic instability, Journal of the Atmospheric Sciences 69 (2012), 1633–1656.

#### Global bifurcation for corotating vortex patches

Susanna V. Haziot

(joint work with Claudia García)

We will consider solutions to the two dimensional incompressible Euler equations, which in the velocity-vorticity formulation, take the form

(1) 
$$\partial_t \omega + (v \cdot \nabla \omega) = 0, \quad v = \nabla^{\perp} \Psi, \quad -\Delta \Psi = \omega.$$

Here,  $\omega$  denotes the vorticity in the fluid, v the fluid velocity and  $\Psi$  the streamfunction. Throughout, we will identify  $(x,y) \in \mathbb{R}^2$  with  $z = x + iy \in \mathbb{C}$ .

Vortex patches are solutions D(t) to (1) consisting of a region of constant vorticity, submerged in an irrotational fluid. Mathematically, these are expressed by

$$\omega(z,t) = 1 \text{ for } z \in D(t), \quad \text{and} \quad \omega(z,t) = 0 \text{ for } z \notin D(t).$$

Due to the structure of the Euler equations, although the boundary of the patch D(t) evolves in time, the area remains fixed. Here, we will focus on vortex pairs, where  $D_1 = -D_2$ , and the goal will be to find solutions which satisfy the initial data

$$\omega_0(z) = \frac{1}{\varepsilon^2 \pi} (\chi_{D_1(0)}(z) + \chi_{D_2(0)}(z)).$$

The reason behind the rescaling of the vorticity is precisely because these pairs of vortex patches will be constructed as a desingularization of point vortices, mathematically represented by delta distributions, and hence we need to allow for patches of different sizes, specifically, of size  $\varepsilon^2$ .

Moreover, we will focus on solutions which are steady, in the sense that they are patches of permanent shape which rotate around each other at constant angular velocity  $\Omega$ . These are referred to as  $corotating\ vortex\ patches$ . By studying these patches in a frame of reference which rotates at the same speed  $\Omega$ , in this frame of references, the patches will appear to be stationary, or steady. Hmidi and Mateu [4] proved the existence of a curve of infinitesimally small such solutions by means of an implicit function argument. These bifurcate from a pair of point vortices where the bifurcation parameter is the radius of the patches  $\varepsilon$ .

The aim is the extend this local curve of solutions to a global one by means of a global bifurcation argument. The solutions obtain through this process will be far away from these infinitesimally small ones on the local curve, and the goal is to reach patches of more interesting shapes. The first, and only other, global bifurcation result for vortex patches was carried out by Hassainia, Masmoudi and Wheeler [3] for the single patch setting.

By expressing (1) in terms of the relative stream function  $\Psi = \psi_0 - \frac{1}{2}\Omega|z|^2$  for  $\Psi \in C^1(\mathbb{C})$  we then get

(2a) 
$$\Delta\Psi = \frac{1}{\varepsilon^2 \pi} \chi_{D_1} + \frac{1}{\varepsilon^2 \pi} \chi_{D_2} - 2\Omega,$$

(2b) 
$$\nabla(\Psi + \frac{1}{2}\Omega|z|^2) \to 0$$
, as  $|z| \mapsto \infty$ , and  $\Psi = c_m$ , on  $\partial D_m$ ,

for some constants  $c_m$ , m=1,2. Since both the  $D_m$  and the function  $\Psi$  are unknowns, this is a free boundary problem. We obtain the following result.

**Theorem 1.** [1] There exists a continuous curve C of corotating vortex patch solutions to (2), with graphical boundary  $R(\theta)e^{i\theta}$ , parameterized by  $s \in (0, \infty)$  along which:

- i) (Bifurcation from point vortex) As  $s \to 0$  the solution limits to the point vortex pairs.
- ii) (Limiting configurations)  $As s \to \infty$

$$\min \left\{ R'(\theta), \min_{\partial D_1} \varepsilon \nabla \psi(z), \min_{z_m \in \partial D_m} |z_1 - z_2| \right\} \to 0$$

- iii) ( $\varepsilon$  bounded away from 0) The parameter  $\varepsilon(s)$  is bounded away from 0 for all s away from the local curve.
- iv) (Analyticity) For each s > 0, the boundary  $\partial D_m$  is analytic.

The first limiting configuration indicates that the polar graph condition fails, suggesting star-shaped patches. The second limiting configuration suggests the presence of corners along the boundary of the patches, and the third one means the boundaries of the two patches intersect. Numerics [5] suggest that the only limiting configuration which can take place is the two patches intersecting, with a corner at the point of intersection. This is known as Overman's conjecture, and the proof is still a major open problem in the field.

The third point in the theorem is a very important result. It guarantees that the global curve cannot end at a pair of point vortices anywhere other than along the local curve of solutions. The core of the proof relies on the following rigidity theorem.

**Theorem 2.** [1] If  $\omega_0 = (\pi \varepsilon^2)^{-1} (\chi_{D_1} + \chi_{D_2})$  is a solution to the vortex pair problem then  $\Omega \in (0, 1/(2\pi \varepsilon^2))$ . Moreover, if  $\varepsilon \leq l/10$  then  $|\Omega| \lesssim |l|^{-2}$ , where l is the distance of the center of the patch  $D_1$  to the y-axis.

The first part of the theorem is an adaptation of the result in [2] to the twopatch setting. The second part is new with the striking property that it provides uniform bounds on  $\Omega$  regardless of where along the global curve the solution lies.

#### References

- C. García, S.V. Haziot Global bifurcation for corotating and counter-rotating vortex pairs, Comm. Math. Phys. 402 (2017), no.2, 1167–1204.
- [2] J. Gómez-Serrano, J. Park, J. Shi, Y. Yao Symmetry in stationary nd uniformly rotating solutions of active scalar equations, Duke Math. J. 170 (2021), no.13, 2957–3038.
- [3] Z. Hassainia, N. Masmoudi, M.H. Wheeler Global bifurcation of rotating vortex patches, Comm. Pure Appl. Math. 73 (2020), no.9, 1933–1980.
- [4] T. Hmidi, J. Mateu Existence of corotating and counter-rotating vortex pairs for active scalar equations, Comm. Math. Phys. **350** (2017), no.2, 699–747.
- [5] H.M. Wu, E.A. Overman II, N.J. Zabusky Steady-state solutions of the Euler equations in two dimensions:rotating and translating V-states with limiting cases. I. Numerical algorithms and results, J. Comput. Phys. 53 (1984), no.1, 42–71.

## Two-dimensional turbulence above topography: condensation transition and selection of minimum enstrophy solutions

#### Basile Gallet

Two-dimensional turbulence above topography is a fascinating system to test the predictive skill of large-scale organizing principles for high-Reynolds-number flows. Among those principles are the statistical physics of two-dimensional flows, and the selective decay assumption. In the present context, the latter principle states that enstrophy should be minimized while conserving the initial value of the energy [1].

In the present study we focus on a 2D turbulence in a doubly periodic domain, above smaller scale topography, within the quasi-geostrophic approximation. The topography is at a scale strictly smaller than the domain size, although no scale separation is required. We revisit selective decay for this setup and highlight a new branch of solutions to the variational problem, which corresponds to a large-scale 'condensate', that is, a large-scale circulation arising at the domain scale. For weak initial energy, we predict that the flow organizes at the scale of the topography, with no large-scale condensate. When the initial energy exceeds a threshold value, a large-scale condensate emerges. At large initial energy, the system thus displays the typical large-scale condensates that have been reported for two-dimensional turbulence without topography [2]. We compare the theoretical prediction for the amplitude of the condensate with numerical simulations of the system using pseudo-spectral methods and a small hyperviscosity. Very good quantitative agreement is obtained.

A second question of interest is whether such variational principles can be extended to out-of-equilibrium systems. Indeed, real flows are often forced and dissipative, whereas the variational principles have been designed for energy-conserving systems. How to extend selective decay to the forced-dissipative situation? We provide an answer to this question in the regime where the forcing and damping (linear friction) are small, using a perturbative expansion. To lowest order, we recover the energy-conserving system. Leveraging selective decay, we predict that the system is on the condensed branch, the amplitude of the condensate being undetermined at this stage. Through a solvability condition arising at next order in the expansion, we obtain a governing equation for the slow evolution of the amplitude of the condensate, akin to the normal form of a standard bifurcation. We first solve this equation for a forcing that is spatially correlated with the structure of the bottom topography, predicting a continuous transition to condensation as the forcing strength exceeds a threshold value. We then consider the situation where the forcing is at the domain scale, predicting a discontinuous transition to condensation as the forcing strength increases. We have performed pseudo-spectral simulations of the forced-dissipative system, obtaining very good quantitative agreement with the predictions for both types of forcing. Some slight discrepancy arises very near the instability threshold. This discrepancy seems to stem from the presence of isolated vortices pinned to the topography, which are not predicted by selective decay.

This work suggests a large-scale organizing principle for some weakly out-of-equilibrium systems [3]. However, many questions remain, among which:

- The present numerical simulations were performed with single-scale topography, but the theory holds for any topography. It would be interesting to investigate whether the observed agreement between theory and numerics remains for more complex topography.
- It would also be desirable to understand the physical origin of the vortices that are pinned to the topography. Can the theory be extended to predict their strength and location?

#### References

- F.P. Bretherton, D.B. Haidvogel, Two-dimensional turbulence above topography, J. Fluid Mech. 78 (1976), 129–154.
- [2] B. Gallet, W.R. Young A two-dimensional vortex condensate at high Reynolds number, J. Fluid Mech. 715 (2013), 359-388.
- [3] B. Gallet, Two-dimensional turbulence above topography: condensation transition and selection of minimum enstrophy solutions, J. Fluid Mech. 988 (2024), A13.

## Optimal Balance - A black-box method for fast-slow decompositions of fluid flow

#### Marcel Oliver

Many equations of geophysical fluid dynamics can be considered as a fast-slow system of the form

$$\dot{q} = F(q, p)$$

(1b) 
$$\varepsilon \, \dot{p} = Jp - G(q, p)$$

where J is a skew operator. In many cases, it is possible to show existence of a slow manifold  $p = \Phi(q)$  such that the reduced equation  $\dot{q} = F(q, \Phi(q))$  approximates a solution of the full system with well-prepared initial data. This type of slow manifold is typically neither invariant nor unique, but can often be constructed by asymptotic expansion to arbitrarily high order [4]. For finite dimensional Hamiltonian examples, an optimal truncation of the associated asymptotic series gives exponential accuracy over long times.

Optimal balance is a method that constructs one point on the slow manifold computationally to high accuracy, without the need to compute and implement asymptotic expansions. It requires a modification of the fast-slow system, where the nonlinear terms can be gently turned on by way of a "ramp function"  $\rho(\tau)$  that satisfies  $\rho(0) = 0$  and  $\rho(1) = 1$ . For accuracy at order  $O(\varepsilon^n)$ , we further require that all derivatives up to order n vanish at the two endpoints of the ramp. Optimal truncation even requires that all derivatives of  $\rho$  vanisch at the two endpoints. Then,  $\rho$  can be at best in some quasi-analytic class of functions.

Given  $\rho$ , we solve the boundary value problem in time,

(2a) 
$$\dot{q} = \rho(t/T) F(q, p)$$

(2b) 
$$\varepsilon \, \dot{p} = Jp - \rho(t/T) \, G(q, p)$$

with the "linear end" boundary condition p(0) = 0, which indicates that at the initial time, when the system is linear, the system state is exclusively slow, and the "nonlinear end" boundary condition  $q(T) = q^*$  which fixes the base point at which we want to compute the slow manifold. Then  $\Phi(q^*) \approx p(T)$  is an approximation to the slow manifold.

The idea behind optimal balance is the adiabatic invariance of slow manifolds under slow homotopies, which goes back to ideas developed in the early days of quantum mechanics (e.g. [1]), appeared many times in different field of mechanics and was introduced in the present context as "optimal vorticity balance" by [6].

We have the following theorem, proved in [3] in finite dimensions for systems with a particular Hamiltonian structure.

**Theorem 1.** Suppose F, G are analytic,  $\rho \in G^2$  with  $\rho(0) = 0$ ,  $\rho(1) = 1$ ,  $\rho^{(i)}(0) = \rho^{(i)}(1) = 0$  for  $i \geq 1$ . Then there exist constants c and d so that for all  $\varepsilon > 0$ 

(3) 
$$||p(T) - \Phi(q^*)|| \le d \exp\left(-\frac{c}{\varepsilon^{1/3}}\right)$$

where (q,p) solve the boundary problem (2) and  $\Phi$  denotes the mapping that represents a slow manifold obtained by asymptotically optimal truncation.

This result raises two questions: Is the optimal balance formulation (2) even well-posed, and if so, how can we compute the solution. An obvious strategy, already used in the numerical implementation of [6], is "backward-forward nudging". Here, the optimal balance differential equation is solved alternatingly as a forward resp. backward initial value problem between t=0 and t=T. At the linear end, p(0)=0 is imposed before changing direction of integration, at the nonlinear end,  $q(T)=q^*$  is imposed before again changing direction of integration. The following theorem, proved in [5] in the same framework as the previous theorem, shows that this process converges up to an exponentially small remainder:

**Theorem 2.** Under the same conditions as Theorem 1, for every T there are constants C and D so that

(4) 
$$\limsup_{m \to \infty} \|p_m^+(T) - \Phi(q^*)\| \le D \exp\left(-\frac{C}{\sqrt[3]{\varepsilon}}\right)$$

for all  $\varepsilon$  sufficiently small, where m denotes the count of nudging iterations, and  $p_m^+(T)$  is the final value of the p-component in the forward integration.

This theorem shows that the boundary value problem is well posed up to possibly an exponentially small residual. Further, it shows that the nudging error is asymptotically as small as the optimal balance error of Theorem 1.

The main advantage of optimal balance is that it can be implemented in existing computational models with only minor modifications: we need to insert the time-dependent ramp function before all nonlinear terms, and we need to be able to reverse the direction of integration. (Typical eddy viscosities do not make a significant difference in practice due to the small time horizon of the integration, but of course viscosities need to be dissipative in the time direction of integration.) Practical tests show, in the context of the f-plane shallow water equations that optimal balance is highly effective and competitive with high-order asymptotic methods. Moreover, for actual numerical code, the notion of balance is closely tied to the concrete numerical scheme at this level of accuracy [2].

Current work is progressing toward using optimal balance in more realistic settings, namely three-dimensional equations, fluid dynamics on the mid-latitude  $\beta$ -plane, on the equatorial  $\beta$ -plane, and on the sphere. Initial results show that in order to avoid the need to formulate a projection onto the linear slow modes, which may be very difficult in general settings, we can extend the idea of adiabatic

invariance by also changing the linear operator adiabatially, such that slow modes at the linear end of the ramp are always stationary, thus easily computable.

#### References

- [1] M. Born and V. Fock, Beweis des Adiabatensatzes, Z. Physik 51 (1928), 165–180.
- [2] M. Chouksey, C. Eden, G. T. Masur, and M. Oliver, A comparison of methods to balance geophysical flows, J. Fluid Mech. 971 (2023), A2.
- [3] G.A. Gottwald, H. Mohamad, and M. Oliver, Optimal balance via adiabatic invariance of approximate slow manifolds, Multiscale Model. Simul. 15 (2017), 1404–1422.
- [4] R.S. MacKay, Slow manifolds, in Energy Localisation and Transfer, T. Dauxois, A. Litvak-Hinenzon, R.S. MacKay, and A. Spanoudaki, eds., World Scientific, 2004, pp. 149–192.
- [5] G.T. Masur, H. Mohamad, and M. Oliver, Quasi-convergence of an implementation of optimal balance by backward-forward nudging, Multiscale Model. Simul. 21 (2023), 624– 640.
- [6] Á. Viúdez and D.G. Dritschel, Optimal potential vorticity balance of geophysical flows, J. Fluid Mech. 521 (2004), 343–352.

## Inviscid incompressible convection in porous media: nonlinear Helmholtz decomposition, combinatorics and relaxed equations

#### Yann Brenier

In the simplest case, incompressible convection in a porous medium  $D \subset \mathbb{R}^d$  may be written in Lagrangian coordinates:

$$\frac{dX_t}{dt}(a) = G(a) - (\nabla p)(t, X_t(a)), \ a \in D.$$

Here  $X_t$  is a volume-preserving map of D,  $\forall t \geq 0$ , and G is a "buoyancy" force (typically  $G(a) = (0, 0, \rho_0(a))$  as d = 3).

The Eulerian version (a.k.a. incompressible porous medium or Muskat equations) easily follows when  $X_t$  is assumed to be a diffeomorphism and  $X_0(a) = a$ . Indeed, let us define implicitly the velocity field v and the "buoyancy" field g

$$\frac{dX_t}{dt}(a) = v(t, X_t(a)), \quad g(t, X_t(a)) = G(a), \quad a \in D.$$

We easily get  $(\partial_t + v \cdot \nabla)g = 0$ . Since  $X_t$  is volume preserving, v is automatically divergence free and parallel to  $\partial D$ . Finally,  $v = g - \nabla p$ . This exactly means that v is the Helmholtz  $L^2$  projection of g onto divergence-free fields parallel to  $\partial D$ .

Time discretization by polar factorization. Let us recall the polar factorization theorem for maps (Y.B. 1987/91-Euclidean case, R. McCann 2001-Riemannian case) that can be seen as a nonlinear version of the Helmholtz decomposition theorem.

**Theorem 1** ([1]). Let  $D \subset \mathbb{R}^d$  be a compact domain. Then, any non degenerate  $T \in L^2(D,\mathbb{R}^d)$  (i.e.  $\forall N \subset \mathbb{R}^d$ ,  $vol(N) = 0 \Rightarrow vol(T^{-1}(N)) = 0$ ) admits a unique factorization  $T = \nabla U \circ X$ , where  $U : \mathbb{R}^d \to \mathbb{R}$  is convex and  $X : D \to D$  is volume-preserving (i.e.  $vol(X^{-1}(W)) = vol(W)$ ,  $\forall W \subset D$ ). In addition, as d = 1,  $\nabla U$  is just the increasing rearrangement of T.

To discretize the Muskat system

$$\frac{d}{dt}X_t(a) = G(a) - (\nabla p)(t, X_t(a)) ,$$

with time step  $\delta t$ , we polar factorize, at each time step n, the "predictor"  $X^n + \delta t$  G as  $\nabla U^{n+1} \circ X^{n+1}$ , with  $X^{n+1} : D \to D$  volume preserving,  $U^{n+1}$  convex.

This "predictor-corrector" scheme still makes sense in 1D and can be trivially coded using permutations [2] while 2D simulations have been very recently performed (Bruno Lévy, personal communication) thanks to Quentin Mérigot's semi-discrete optimal transport solver.

Multiphasic ("Young's measure") reformulation. (Y.B. Chin. Ann. Math '09, hidden convexity book '20 https://hal.science/hal-02928398)

$$\frac{dX_t}{dt}(a) = G(a) - (\nabla p)(t, X_t(a))$$

translates in terms of  $c(t, x, a) = \delta(x - X_t(a))$  into a pseudo-differential system of conservation laws:

$$\partial_t c(t, x, a) = \nabla_x \cdot (c(t, x, a)[-G(a) + \nabla p(t, x)])$$

 $\Delta p(t,x) = \nabla_x \cdot \left( \int_a c(t,x,a) G(a) \right)$ . This is somewhat surprising since the Muskat equations are often considered as a gradient flow (as in Otto's work)!

Note that  $c(\cdot,\cdot,a)\geq 0$  is the concentration of phase a which can now be a DISCRETE label. In 1D, the 2-phase case  $a\in\{0,1\}$  corresponds to the inviscid Burgers equation (a.k.a Buckley-Leverett equation, as in Otto CPAM '99 or Székelyhidi Ann. ENS '12), while the 3 phase case  $a\in\{0,1,2\}$  gives the Le Roux equations

(a not so known  $2 \times 2$  system of hyperbolic conservation laws cf. D. Serre's book), which can be also derived from a stochastic model as in J. Fritz-B. Tóth '04:  $\partial_t \rho + \partial_x (\rho u) = 0$ ,  $\partial_t u + \partial_x (u^2 + \rho) = 0$  (N.B.  $u^2$  not  $u^2/2$ !). These formulations are well suited for standard upwind finite difference schemes that we may therefore compare with the "permutation scheme" discussed above (and based on the polar factorization theorem for maps).

Entropy conservation and local well-posedness. The multiphasic formulation of the Muskat system

$$\partial_t c(t, x, a) = \nabla_x \cdot (c(t, x, a)[-G(a) + \nabla p(t, x)]), \quad \Delta p(t, x) = \int_a \nabla_x \cdot (c(t, x, a)G(a))$$

admits an extra conservation law for the Boltzmann entropy  $\int_{x,a} c \log c$ , which is strictly convex in c. This essentially suffices for local well-posedness (cf. Dafermos' book on systems of conservation laws and work in progress with E. Stämpfli, to deal with the pseudo-differential part when d > 1.)

Toward a "gradient flow" formulation? We have,

$$\begin{split} \frac{d}{dt} \int_{x,a} |x - G(a)|^2 c(t,x,a) &= 2 \int_{x,a} (x - G(a)) \cdot m(t,x,a) \\ &= 2 \int_{x,a} (\nabla p(t,x) - G(a)) \cdot m(t,x,a) \\ &= \int_{x,a} -\frac{|m(t,x,a)|^2}{c(t,x,a)} - |G(a) - \nabla p(t,x)|^2 c(t,x,a) \\ &+ \frac{|m(t,x,a) - (G(a) - \nabla p(t,x))c(t,x,a)|^2}{c(t,x,a)}. \end{split}$$

for ANY smooth

$$(t, x, a) \rightarrow (c(t, x, a), m(t, x, a), \nabla p(t, x)) \in \mathbb{R}_+ \times (\mathbb{R}^d)^2$$

such that

$$\int_{a} c(t, x, a) = 1, \quad \partial_{t} c(t, x, a) + \nabla \cdot m(t, x, a) = 0, \quad (\Rightarrow \int_{a} \nabla \cdot m(t, x, a) = 0).$$

This suggests the "gradient flow" formulation of the multiphasic Muskat equations:

$$\frac{d}{dt} \int_{x,a} |x - G(a)|^2 c(t, x, a) + \int_{x,a} \frac{|m(t, x, a)|^2}{c(t, x, a)} + |G(a) - \nabla p(t, x)|^2 c(t, x, a) \le 0$$
s.t. 
$$\int_a c(t, x, a) = 1, \quad \partial_t c(t, x, a) + \nabla \cdot m(t, x, a) = 0,$$

which is convex in (c, m) but unfortunately not in  $(c, m, \nabla p)$ .

#### References

- [1] Y. Brenier, Polar factorization and monotone rearrangement of vector-valued functions, CPAM (1991).
- [2] Y. Brenier, Various formulations and approximations of incompressible fluid motions in porous media, Ann. Math. Quebec (2022).

Reporter: Antoine Leblond

## **Participants**

#### Prof. Dr. Claude Bardos

Laboratoire Jacques-Louis Lions Université Paris 6 4, Place Jussieu 75252 Paris Cedex 05 FRANCE

#### Daniel Bäumer

Fakultät für Mathematik Universität Wien Oskar-Morgenstern-Platz 1 1090 Wien AUSTRIA

#### **Daniel Boutros**

Department of Applied Mathematics and Theoretical Physics Centre for Mathematical Sciences University of Cambridge Wilberforce Road Cambridge CB3 0WA UNITED KINGDOM

## Dr. Felix Brandt

Department of Mathematics University of California, Berkeley 970 Evans Hall Berkeley CA 94720-3840 UNITED STATES

#### Prof. Dr. Yann Brenier

Laboratoire de Mathematiques d'Orsay, Universite Paris-Saclay Batiment 307, rue Michel Magat 91405 Orsay FRANCE

#### Prof. Dr. Adrian Constantin

Fakultät für Mathematik Universität Wien Oskar-Morgenstern-Platz 1 1090 Wien AUSTRIA

#### Dr. Laura Cope

Department of Mathematics and Statistics Harrison Building Streatham Campus University of Exeter North Park Road Exeter EX4 4QF UNITED KINGDOM

#### Prof. Dr. Anne-Laure Dalibard

Laboratoire Jacques-Louis Lions Sorbonne Université 4, Place Jussieu 75252 Paris Cedex 05 FRANCE

#### Stefan Dingel

Institut für Mathematik Universität Kassel Heinrich-Plett-Straße 40 34132 Kassel GERMANY

#### Prof. Dr. Emmanuel Dormy

Dept. de Mathématiques et Applications École Normale Superieure 45, rue d'Ulm 75005 Paris Cedex FRANCE

## Dr. Jeffrey Early

NorthWest Research Associates 1100 NE 45th St, Suite 500 Seattle, WA 98145-1535 UNITED STATES

#### Dr. Basile Gallet

CEA Saclay Service de Physique de l'Etat Condensé Bât. 772, Orme des Merisiers 91191 Gif-sur-Yvette FRANCE

#### Corentin Gentil

Dept. de Mathématiques et Applications École Normale Superieure 45, rue d'Ulm 75005 Paris 75005 FRANCE

#### Yanqiu Guo

Department of Mathematics and Statistics Florida International University 11200 SW 8th Street, DM 430 Miami FL 33199 UNITED STATES

#### Dr. Susanna Haziot

Department of Mathematics Princeton University Fine Hall, Washington Road Princeton 08544 UNITED STATES

#### Prof. Dr. Matthias Hieber

Fachbereich Mathematik Technische Universität Darmstadt Schloßgartenstrasse 7 64289 Darmstadt GERMANY

#### Dr. Ruiao Hu

Imperial College London
Department of Mathematics
Huxley Building
180 Queen's Gate
London SW7 2AZ
UNITED KINGDOM

#### Prof. Dr. Amru Hussein

FB 17 - Mathematik/Informatik -Universität Kassel Heinrich-Plett-Str. 40 34132 Kassel GERMANY

#### Dr. Lucas Huysmans

Max Planck Institute for Mathematics in the Sciences Inselstrasse 04103 Leipzig CB3 0WA GERMANY

#### Prof. Dr. Slim Ibrahim

Department of Mathematics and Statistics University of Victoria P.O. Box 3060 Victoria BC V8W 3R4 CANADA

#### Prof. Dr. Boualem Khouider

Department of Mathematics and Statistics University of Victoria P.O. Box 3060 Victoria BC V8W 3R4 CANADA

## Prof. Dr. Rupert Klein

Fachbereich Mathematik und Informatik Freie Universität Berlin Arnimallee 6 14195 Berlin GERMANY

## Prof. Dr. Peter Korn

Max Planck Institute for Meteorology, Hamburg Bundesstraße 53 20146 Hamburg GERMANY

#### Prof. Dr. Igor Kukavica

Department of Mathematics University of Southern California, Dornsife KAP 104 3620 S. Vermont Avenue Los Angeles, CA 90089-2532 UNITED STATES

#### Dr. Antoine Leblond

Max Planck Institut für Meteorologie Bundesstr. 53 20146 Hamburg GERMANY

## Prof. Dr. Jinkai Li

South China Research Center of Applied Mathematics and Interdisciplinary Studies
School of Mathematical Sciences
South China Normal University
No. 55, Zhongshan Avenue West
Guangzhou 510631
CHINA

#### Prof. Dr. Yasunori Maekawa

Department of Mathematics Graduate School of Science Kyoto University Kitashirakawa, Oiwake-cho, Sakyo-ku Kyoto 606-8502 JAPAN

#### Dr. Simon Markfelder

Department of Mathematics and Statistics University of Konstanz Postfach 199 78457 Konstanz GERMANY

#### Dr. Carolin Mehlmann

Otto-von-Guericke-Universität Universitätsplatz 2 39106 Magdeburg GERMANY

#### Prof. Dr. Dongjuan Niu

School of Mathematical Sciences, Capital Normal University Xisanhuan North Road 105 Beijing 100 048 CHINA

#### Prof. Dr. Marcel Oliver

Chair of Applied Mathematics Mathematical Institute for Machine Learning and Data Science KU Eichstätt-Ingolstadt Auf der Schanz 49 85049 Ingolstadt GERMANY

#### Prof. Dr. Felix Otto

Max-Planck-Institut für Mathematik in den Naturwissenschaften Inselstraße 22 - 26 04103 Leipzig GERMANY

## Luigi Roberti

Fakultät für Mathematik Universität Wien Oskar-Morgenstern-Platz 1 1090 Wien AUSTRIA

#### Prof. Dr. Leslie M. Smith

Department of Mathematics University of Wisconsin, Madison 480 Lincoln Drive Madison WI 53706-1388 UNITED STATES

## Prof. Dr. Samuel N. Stechmann

Department of Mathematics University of Wisconsin-Madison 480 Lincoln Drive Madison WI 53706-1388 UNITED STATES

#### Dr. Oliver Street

Grantham Institute Imperial College London Exhibition Road, South Kensington London SW7 2AZ UNITED KINGDOM

## Prof. Dr. László Székelyhidi Jr.

Max-Planck-Institut für Mathematik in den Naturwissenschaften Inselstr. 22 - 26 04103 Leipzig GERMANY

## Sophie Thery

Institut für Mathematik Universität Augsburg 86135 Augsburg GERMANY

## Prof. Dr. Marita Thomas

Freie Universität Berlin und Weierstraß-Institut für Angewandte Analysis und Stochastik Arnimallee 9 14195 Berlin GERMANY

#### Prof. Dr. Edriss S. Titi

Department of Applied Mathematics and Theoretical Physics Centre for Mathematical Sciences University of Cambridge Wilberforce Road Cambridge CB3 0WA UNITED KINGDOM

#### Dr. Jörg Weber

Fakultät für Mathematik Universität Wien Oskar-Morgenstern-Platz 1 1090 Wien AUSTRIA

#### Prof. Dr. Mathias Wilke

Martin-Luther-Universität Halle-Wittenberg Naturwissenschaftliche Fakultät II Institut für Mathematik 06099 Halle / Saale GERMANY

#### Da Yang

Department of the Geophysical Sciences University of Chicago 5734 S. Ellis Avenue Chicago IL 60637 UNITED STATES